Grad-Shafranov equation: MHD simulation of the new solution obtained from the Fadeev and Naval models

A. Ojeda-González[1*], L. Nunes dos Santos[1,2†], J.J. González-Avilés[3,4‡], V. De la Luz[5§], and P.R. Muñoz-Gutberlet[6¶]

[1]Instituto de Física e Astronomía, Universidade do Vale do Paraíba-UNIVAP, São José dos Campos, São Paulo, Brazil
[2]Departamento de Matemática, Universidade Federal de Mato Grosso do Sul, Aquidauana - MS, Brazil
[3]CONACyT-Servicio de Clima Espacial México-Laboratorio Nacional de Clima Espacial, SCiESMEX-LANCE, Morelia, Michoacán, México
[4]Instituto de Geofísica, Unidad Michoacán, Universidad Nacional Autónoma de México, Antigua Carretera a Pátzcuaro 8701, 58190, Morelia, Michoacán, México
[5]Escuela Nacional de Estudios Superiores, Unidad Morelia, Universidad Nacional Autónoma de México, 58190, Morelia, Michoacán, México
[6]Departamento de Física e Astronomía, Universidad de La Serena, Av. Juan Cisternas 1200, La Serena, Chile

Key Points:

- The new analytical solution has magnetic field lines with neutral points and singular points.
- This solution enter as initial condition in an MHD simulation by excluding the singular points.
- The MHD simulation shows the fast evolution of magnetic islands into current sheets.
- This is the first report shows the magnetic field polarity inversion related to analytical solution of the GS equation.
- The importance of the direction and amplitude of the magnetic field near the singular points is explained.

*ORCID iD: `https://orcid.org/0000-0002-6312-9026`
†E-mail:leandro.nunes@ufms.br, ORCID iD: `https://orcid.org/0000-0001-5028-6834`
‡E-mail:jjgonzalez@igeofisica.unam.mx, ORCID iD: `https://orcid.org/0000-0003-0150-9418`
§vdelaluz@enesmorelia.unam.mx, ORCID iD: `https://orcid.org/0000-0003-0257-4158`
¶pablocus@gmail.com, ORCID iD: `https://orcid.org/0000-0002-3435-6422`

Corresponding author: Arian Ojeda-González, `ojeda.gonzalez.a@gmail.com`

Abstract

This article aims to obtain a new analytical solution of a specific form of the Grad-Shafranov (GS) equation using Walker's formula. The new solution has magnetic field lines with X-type neutral points, magnetic islands and singular points. The singular points are located on the x-axis. The X-points and the center of the magnetic islands do not appear on the x-axis an island appears at $z > 0$ and the other two at $z < 0$. The aforementioned property allows us to use this solution as an initial condition at $t = 0$ s in an magnetohydrodynamic (MHD) numerical simulation by excluding the singular points of the solution, i.e., the x-axis, and maintaining the magnetic structure of the islands, as well as the X-type neutral points. For this, we numerically solve the equations of the classical ideal MHD in two dimensions using the Newtonian CAFE code. The code is based on high resolution shock capturing methods using the Harten-Lax-van Leer-Einfeldt (HLLE) flux formula combined with MINMOD reconstructor. The MHD simulation shows a very fast dissipation in less than one second of the magnetic islands present in the initial configuration. Almost all structures left the integration region at 13.2 s, and the magnetic field vector reverses its polarity very quickly. In addition, our simulation allows us to observe the fast temporal evolution of the magnetic islands turning into elongated current sheets. As a limitation of the model, the difficulty in relating it to a physical system because of fast temporal evolution is considered.

1 Introduction

The Grad-Shafranov (GS) equation is written in function of Cartesian coordinates in the plane as follows:

$$\frac{\partial^2 A_y}{\partial x^2} + \frac{\partial^2 A_y}{\partial z^2} = -\mu_0 \frac{d}{dA_y}\left(p(A_y) + \frac{B_y^2(A_y)}{2\mu_0}\right), \tag{1}$$

where A_y is the $y-$component of the magnetic vector potential, μ_0 is the permeability of free space, p is the kinetic plasma pressure, and B_y is the $y-$component of the magnetic field (Grad & Rubin, 1958; Shafranov, 1966).

From the physical point of view, this equation characterizes a plasma as a single collisionless fluid, with high conductivity, immersed in a magnetostatic field. It is important to consider an invariant axis ($\partial/\partial y = 0$) when deducing the GS equation, which makes the geometry of the problem 2.5-D (Ojeda-González et al., 2016). The detailed development of the whole physical formulation can be found, for example, in Sonnerup et al. (2006); Ojeda-González et al. (2015); Hu (2017); Teh (2018).

The GS equation can also be written in the axially symmetric configurations in the cylindrical coordinate system (Ambrosino & Albanese, 2005). This notation is most commonly used in the application of this equation to study the confined magnetic field in a Tokamak (Atanasiu et al., 2004). In its original form, equation (1) is a second order partial differential equation that does not have an analytical solution but can be numerically solved as a Cauchy problem or an initial value problem (Sonnerup & Guo, 1996). The authors Sonnerup and Guo (1996) and Hau and Sonnerup (1999) have developed a numerical method for solving (1). The method consists of making a second order approximation in terms of a Taylor series around a generic point $x = x_0$. A rectangular grid XZ must be constructed during the development of the numerical method. This problem is very convenient because the data collected by a satellite, when it crosses a plasma structure in the interplanetary medium or in the magnetosphere, can be used as initial conditions for implementing the solution numerically.

The physical parameters of the plasma that the satellite will need to measure are the following: the speeds, density and temperature of protons and electrons. In addition, the three magnetic field components will be required. In this way, it is possible to simulate the plasma behavior in regions neighboring the satellite where no measurements were taken. This method is known as Grad-Shafranov reconstruction (GSR), and in the literature several successful studies can be found, for example Hu et al. (2004); Lui et al. (2008); Ojeda-González et al. (2017a).

There is another solution method explained by Lackner (1976); Mc Carthy (1999) that basically consists of an algorithm that makes a least squares fitting, considering only one eigenvalue as a nonlinear parameter in the GS equation numerical solution.

In (1), the right hand side term in the derivative argument is related to the plasma transverse pressure (P_t), where

$$P_t(A_y(x,z)) = p(A_y(x,z)) + \frac{{B_y}^2(A_y(x,z))}{2\mu_0}. \tag{2}$$

Depending on the expression that P_t may assume, equation (1) will have an analytical solution. Several examples such as Tokamak's solution, can be found in the literature (Zheng et al., 1996; Mc Carthy, 1999; Atanasiu et al., 2004).

From a physical point of view, however, one must justify the choice of the mathematical expression of P_t. Using plasma kinetic theory, Kan (1973) solved the set of Vlasov-Maxwell equations by considering a velocity distribution expression as a function of the Boltzmann factor from Maxwell-Boltzmann statistics. As a result of using the Boltzmann factor, the P_t parameter is expressed as an exponential function as follows:

$$P_t(x,z) = P_{t_0}\exp(-2\Psi), \tag{3}$$

where Ψ is the normalized magnetic vector potential and P_{t_0} is the transverse pressure when $A_y = 0$ (Schindler, 2006).

The P_{t_0} parameter exists as a consequence of a drift velocity in the y-direction (even though A_y be zero). In the deduction of the distribution function, this drift velocity was considered by Kan (1973); Kan (1979); Yoon and Lui (2005); Ojeda-González et al. (2015).

The physical parameters Ψ and P_{t_0} are expressed as a function of the characteristic length scale L_0 and the magnitude of the asymptotic magnetic field strength B_0, where

$$\Psi(x,z) = \frac{-2}{L_0 B_0} A_y(x,z), \tag{4}$$

and

$$P_{t_0} = \frac{{B_0}^2}{2\mu_0}. \tag{5}$$

The previous expressions are replaced inside (1) to obtain a specific form of the GS equation as follows:

$$\frac{\partial^2\Psi}{\partial X^2} + \frac{\partial^2\Psi}{\partial Z^2} = \exp(-2\Psi), \tag{6}$$

where a change of variables, $X = x/L_0,\ Z = z/L_0$, is performed to normalize x and z, transforming X and Z into dimensionless quantities. In the mathematical formulation adopted here, the $y-$component of the current density J_y is as follows:

$$J_y(x,z) = \frac{B_0}{L_0\mu_0}\exp(-2\Psi). \tag{7}$$

The mathematical expression given by (6) has the form of a Poisson's equation. In the specific case where the inhomogeneous term adopts an exponential form, however, the equation is now called the two-dimensional Liouville equation, which in its original form is written $\Phi_{xx} + \Phi_{yy} = c\exp(d\Phi)$ with c and d being real constants (Biskamp, 1986; Schindler, 2006).

By considering complex variables $\zeta = x + \iota y$ and $\overline{\zeta} = x - \iota y$, the problem goes to the complex plane where the equivalent function $\Phi_{\zeta\overline{\zeta}} = (c/4)\exp(d\Phi)$ must be solved as explained by Crowdy (1997). In the development of the solution presented by Stuart (1967); Biskamp (1986); Schindler (2006), the general solution of the Liouville equation has been parameterized by an analytical function, $g(\zeta) = u(x,y) + iv(x,y)$, where $g(\zeta)\overline{g}(\overline{\zeta}) = u^2(x,y) + v^2(x,y)$ and $g'(\zeta)\overline{g}'(\overline{\zeta}) = u_x^2(x,y) + u_y^2(x,y)$ with $d = -2$ e $c = 1/4$, obtaining the Liouville solution:

$$\Phi(x,y) = \ln\left[\frac{1 + |g(\zeta)|^2}{2\left|\frac{dg}{d\zeta}\right|}\right]. \tag{8}$$

Adapting this generic solution to the initial problem given by (6), a wide variety of generating functions $g(\xi)$ (with $\xi = X + \iota Z$ as a dimensionless complex quantity) could be obtained, with a domain in the set of complex numbers that can offer Ψ solutions in the set of real numbers. The formula to obtain general solutions is written as follows:

$$\Psi(X,Z) = \ln\left[\frac{1 + |g(\xi)|^2}{2|g'(\xi)|}\right], \tag{9}$$

with $g'(\xi) = dg(\xi)/d\xi$.

It is also important to note that some authors in the area of space physics (A. V. Manankova & Pudovkin, 1996, 1999; A. Manankova et al., 2000; A. V. Manankova, 2003; Yoon & Lui, 2005; Korovinskiy et al., 2018) called (9) Walker's formula (Walker, 1915). Following the previous convention in the rest of this article, equation (9) will also be called Walker's formula.

It is worth highlighting the suggestion of Génot (2005) and rewriting (6) as

$$\Delta\Psi = -\Delta \ln[|g'(\xi)|] + \frac{4|g'(\xi)|^2}{[1 + |g(\xi)|^2]^2}, \tag{10}$$

where Δ represents the Laplacian operator.

The importance of equation (10) is that it allows determining the singular points (X,Z) of $\Psi(X,Z)$ calculating poles and zeros of $g'(\zeta)$ (Génot, 2005). That is, singularities can be directly determined from Ψ or from the zeros and poles of $g'(\zeta)$ (Yoon & Lui, 2005b).

The usefulness of having analytical solutions is that, for example, (1) does not have an analytical solution but can be numerically solved as a Cauchy problem, and the differential equation is subject to certain initial conditions (Sonnerup & Guo, 1996; Hau & Sonnerup, 1999; Hu & Sonnerup, 2001; Ojeda-González et al., 2015). In the work of Hau and Sonnerup (1999), an analytical solution of (6) proposed by Fadeev et al. (1965) was used to create a contour plot that allowed the visualization of the percentile error, useful in quantifying the quality during the numerical solution development. New analytical solutions from (6) obtained from (9) may also be important for validating future improvements in the numerical solution.

Analytical solutions are also important for understanding the coexistence between the X-type (where magnetic reconnection can happen), O-type (magnetic island), and S-type points (S for singular) which appear for example in the Kan model (Kan, 1979). Furthermore, the analytical solution was found by Laurindo-Sousa et al. (2018).

Another application of analytical solutions may be their use as initial conditions in magnetohydrodynamic (MHD) and electromagnetic particle in cell (PIC) simulations (Birn & Hesse, 2001). These simulations were intended to study the Hall effect on the generalized Ohm's law and the effect of resistivity on the diffusion region of electrons and ions at an X-type neutral point. For example, the Harris solution (Harris, 1962) was used as an initial condition in several articles (Birn & Hesse, 2001; Hesse et al., 2001; Otto, 2001; Shay et al., 2001; Ma & Bhattacharjee, 2001; Pritchett, 2001; Kuznetsova et al., 2001; Becker et al., 2001; Arzner & Scholer, 2001; J. González-Avilés & Guzmán, 2018), whose challenge was to study the two-dimensional magnetic reconnection in the environmental geospace by doing several simulations with different models, performed with the same input parameters.

This article aims to propose a new generating function deduced from the combination of two existing functions in the literature. With the generating function in hand, Walker's formula is used to find a new solution of $\Psi(X, Z)$. Subsequently, by entering this new solution as an initial condition in an MHD model, the plasma evolution in this magnetic configuration is studied.

The article has been structured in such a way as to propose an explicit construction of all theory and arguments that will be approached that give the reader a better understanding. In Section 2, the mathematical equation of Fadeev's solution (Fadeev et al., 1965) is presented. Section 3 presents a transformation of the original solution proposed by Laurindo-Sousa et al. (2018). Section 4 provides a new solution as a result of merging the solutions presented in Sections 2 and 3. Section 5 compares the three aforementioned analytical solutions. In Section 6, the behavior of the new solution has been studied when it is inserted as an initial condition to an MHD model. In Section 7, we discuss the results, and Section 8 shows the summary and conclusions of the article.

2 Fadeev Solution

One of the best known and most used solutions in the literature was proposed by Fadeev in 1965 (Fadeev et al., 1965). Considered a generating function

$$g(\xi) = f_p + \sqrt{(1 + {f_p}^2)}\exp(\iota b \xi), \tag{11}$$

it obtains the following solution:

$$\Psi(X, Z) = \ln\left[f_p \cos(bX) + \sqrt{1 + f_p^2}\cosh(bZ)\right], \tag{12}$$

where b is a scale parameter. The $f_p \in \mathbb{R}$ parameter has the ability to change the size of the magnetic islands observed in the solution graph. Equation (12) has no singular points; this facilitates its usefulness in numerical models by supplying the input parameters (Hau & Sonnerup, 1999; Ojeda-González et al., 2016).

3 NAVAL solution

For the NAVAL[1] solution proposed by Laurindo-Sousa et al. (2018), which transforms the generating function by using a hyperbolic sine ($g(\xi) = \sinh(ib\xi)$) instead of hyperbolic cosine, the solution is given by

$$\Psi(X, Z) = \ln \frac{\cosh^2(bZ) + \sin^2(bX)}{2b\sqrt{\cosh^2(bZ) - \sin^2(bX)}}. \tag{13}$$

The imaginary unit i in the argument of the hyperbolic sine has been used to rotate the solution to an angle of $\pi/2$.

Equation (13) has X-type neutral points, magnetic islands and singular points, respectively. Another solution with similar characteristics regarding the existence of X-points and singular points was proposed by Kan in 1973 (Kan, 1973) and which has been

[1] Nilson-Arian-Virgínia-Alan-Lucas

extensively studied by many authors who also include magnetic islands (A. V. Manankova & Pudovkin, 1996, 1999; A. Manankova et al., 2000; A. V. Manankova, 2003; Yoon & Lui, 2005; Korovinskiy et al., 2018).

4 Proposed solution

One of the aims of this paper is to obtain a new analytical solution by combining the generating functions of Fadeev and NAVAL. The idea is to replace the NAVAL generating function instead of the exponential function of Fadeev's generating function, resulting in

$$g(\xi) = f_p + \sqrt{1+f_p^2}\,\sinh(ib\xi). \tag{14}$$

With the generating function defined, the modulus of the function (14) and first derivative are calculated as follows:

$$|g(\xi)|^2 = f_p^2 - 2f_p\sqrt{1+f_p^2}\cos(bX)\sinh(bZ) + (1+f_p^2)[-\cos^2(bX)+\cosh^2(bZ)], \tag{15}$$

and

$$|g'(\xi)| = \sqrt{(1+f_p^2)b^2[\cosh^2(bZ)-\sin^2(bX)]}. \tag{16}$$

Therefore, by replacing (16) and (15) in Walker's formula (9) and developing some algebraic steps, the new solution is

$$\Psi(X,Z) = \ln\left(\frac{\left(1+f_p^2\right)\left(\cosh^2(bZ)+\sin^2(bX)\right) - 2f_p\sqrt{1+f_p^2}\cos(bX)\sinh(bZ)}{2b\sqrt{\left(1+f_p^2\right)\left(\cosh^2(bZ)-\sin^2(bX)\right)}}\right). \tag{17}$$

By setting $f_p = 0$, the NAVAL solution (13) is recovered.

Using Génov's method cited in the introduction of this article, it is found that (17) has singular points. Génov found a simple method for locating singularities without necessarily solving the equation: without having to calculate derivatives and creating all algebraic manipulations. To do so, singularities can be determined only by

$$|g'(\xi)| = 0. \tag{18}$$

The first derivative of the generating function (14) is $g'(\xi) = ib\sqrt{1+f_p^2}\cos(b\xi)$, and by considering (18), the following expression is found:

$$|g'(\xi)| = b\sqrt{(1+f_p^2)\cos(b\xi)\cos(b\bar{\xi})} = 0. \tag{19}$$

Note that (19) must be zero, but b and $(1+f_p^2)$ are not null. Therefore as it is a product, $\cos(b\xi)$ or $\cos(b\bar{\xi})$ must be null. Singularity points should appear where the cosine nulls: the real part of $b\xi$ must equal to $\frac{\pi}{2}+k\pi$, where $k \in \mathbb{Z}$ and π is given in radians.

5 Relationship between the aforementioned solutions

Figure 1 shows the stream plot of the magnetic field vector at xz-plane superimposed on a background density plot of J_y. The three panels show the following solutions: (a) Fadeev (as in (12)), (b) NAVAL (as in (13)), and (c) our proposal (as in (17)).

Panel (a) is characterized by having an X-type neutral point at the origin of the coordinate system, and in nearby $x > 0$ there is a magnetic island, then an X-point, again an island and so on. This setting repeats itself periodically to infinity. For $x <$

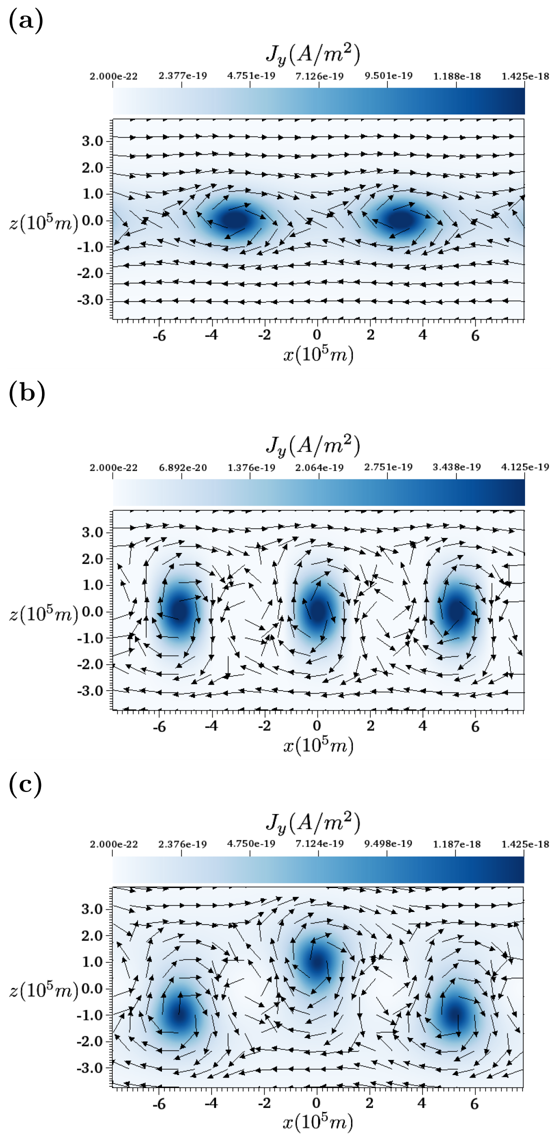

Figure 1. Stream plot of the magnetic field vector $\vec{B}_{xz} = B_x\hat{i} + B_z\hat{k}$ as a function of x and z, superimposed on a background density plot of the scalar field J_y. Panel (a) shows Fadeev's solution from (12). Two magnetic islands are observed and one X-point. Panel (b) shows the NAVAL solution from (13). Panel (c) shows the proposed solution from (17). In both panels (b) and (c), three magnetic islands are observed, as well as two singular points and four X-points, respectively.

0, the setting is exactly the same: there is a symmetry of the solution with respect to the z-axis. The direction of magnetic field rotation in the magnetic islands is clockwise. In panel (b), three O-type points appear on the x-axis, and two S-type singular points are observed between them. There are also four X-type neutral points at the top and bottom of the singular points. Panel (c) shows a configuration similar to panel (b); however, in this case, the center of the magnetic islands does not appear on the x-axis. An island appears at $z > 0$ and the other two at $z < 0$, respectively. Another important detail shown in panels (b) and (c) is the direction of the magnetic field rotation in the magnetic islands (clockwise) relative to the singular points (counterclockwise). The major advantage of the new solution compared with the NAVAL solution is the displacement of the center of the x-axis magnetic islands. This allows us to use this solution in a numerical simulation by excluding the singular points of the solution, i.e., the x-axis, and maintaining the magnetic structure of the islands, as well as the X-type neutral points.

At the moment, no real physical system has been found in which magnetic configurations exist, as shown in Figures 1b and 1c. Therefore, the importance of this study is the mathematical proposal of this new solution and our curiosity about how it evolves in an MHD model as presented in the next section. The motivation for studying the temporal evolution of this system is that the initial configuration (as in Figure 1c) shows a complex structure where magnetic islands and X-type neutral points are present. Regarding the new solution, there are four questions that will be answered in the next sections: (i) How will this configuration evolve in a numerical and dynamic environment? (ii) Will this configuration be temporally stable enough to be observed in any real physical system? (iii) As with the Harris and Fadeev model, can this model be used to study a two-dimensional magnetic reconnection and current sheets? (iv) In addition, how important are the singular points in this model?

6 MHD simulation

In this section, we mention the system of equations and the numerical methods used to perform the simulation of the initial conditions defined in terms of (17). We numerically solve the equations of classical ideal MHD in two dimensions using the Newtonian CAFE code (J. J. González-Avilés et al., 2015; J. González-Avilés & Guzmán, 2018). In particular, the ideal MHD equations are solved on a single uniform cell-centered grid using the method of lines with a third-order Runge-Kutta time integrator. In order to use the method of lines, the MHD equations are discretized using a finite volume approximation with high resolution shock capturing methods. For this, we first reconstruct the variables at cell interfaces using the MINMOD limiter (Harten et al., 1997). On the other hand, the numerical fluxes are built with the Harten-Lax-van Leer-Einfeld (HLLE) approximate Riemann solver formula (Harten et al., 1983; Einfeldt, 1988).

The numerical evolution of initial data involving Maxwell equations leads to the violation of the divergence free constraint equation, developing as a consequence unphysical results like the presence of a magnetic net charge. Among the several methods available for controlling the growth of the constraint violation (Tóth, 2000), in our simulation we use the extended generalized lagrange multiplier (EGLM) method (Dedner et al., 2002).

6.1 Initial conditions

The MHD equations are solved as an initial value problem. For this reason we define the set of initial conditions corresponding to the variables derived from (17). Following Ojeda-González et al. (2015), the expressions for the magnetic field components

B_x, B_y, and B_z in terms of Ψ are

$$\begin{aligned} B_x &= B_0\frac{\partial\Psi}{\partial Z}, & (20)\\ B_y &= B_0\sqrt{\frac{\exp{(-2\Psi)}}{3}}, & (21)\\ B_z &= -B_0\frac{\partial\Psi}{\partial X}. & (22) \end{aligned}$$

The plasma pressure is also defined in terms of Ψ as follows:

$$p = \frac{{B_0}^2}{3\mu_0}\exp{(-2\Psi)}. \tag{23}$$

For this simulation, the mass density ρ is obtained through the equation of state of an ideal gas:

$$p = \frac{k_B\rho T}{\bar{m}}, \tag{24}$$

where k_B is Boltzmann's constant, T is the temperature, $\bar{m}$ is the mean particle mass defined in terms of the mean atomic weight μ through $\mu = \bar{m}/m_p$, where m_p is the proton's mass. For this article, we fixed the value of temperature to $T = 10^7$ K, which is a typical value of the magnetospheric conditions. In addition μ =0.6, this is a value for a fully ionized plasma. Therefore, mass density is defined as follows:

$$\rho = \frac{\bar{m}p}{k_BT} = \frac{\bar{m}B_0^2}{3k_BT\mu_0}\exp{(-2\Psi)}. \tag{25}$$

In this case we consider at initial time the velocity components v_x, v_y and v_z equal to zero.

To perform the numerical simulation, the set of MHD equations are rescaled i.e., the equations become dimensionless, which helps to avoid the appearance of dominant numerical factors during the solution. In this article, we follow the conventions used in J. J. González-Avilés and Guzmán (2015) and fix the scale factors to the typical values observed in regions of the magnetospheric current sheet, i.e., the length-scale $L_0 = 10^5$ m, the plasma density $\rho_0 = 8.360\times10^{-22}$ g/m^3 and the magnetic field scale $B_0 = 4.915\times 10^{-8}$ T (Kan, 1973). With the previous values, the unit of time is fixed in terms of Alfvén speed ($v_0 = v_{A,0} = \frac{B_0}{\sqrt{\mu_0\rho_0}}$ =1.5×10^6 m/s), which implies $t_0 = L_0/v_0$ =0.066 s. The factor $p_0 = \rho v_0^2$=1.9×10^{-9} Pa, and it is used to normalize the initial condition for gas pressure.

6.2 MHD results

In this section, we analyze the results of the numerical simulations. In particular we show the results of the evolution of the initial conditions defined in the previous section. To perform the numerical simulation of the proposed solution given by the configuration described in panel (c) of Figure 1, we separate the full domain into two parts: i) ($z > 0$), $x \in$[-8.0, 8.0] and $z \in$[0.1, 8.1], ii) ($z < 0$), $x \in$[-8.0, 8.0] and $z \in$[-8.1, 0.1]. The separation is done to avoid the singularity in zero of the magnetic field components B_x (equation (20)) and B_z (equation (22)).

For the first part of the domain ($z > 0$), we perform the simulation of i) that we cover with 200×100 cells. We use a constant Courant factor CFL=0.001, and impose open boundary conditions on all sides.

In Figure 2, we show snapshots of the y-component of the current density J_y with magnetic field vectors at different times. For example, at the initial time we can see a

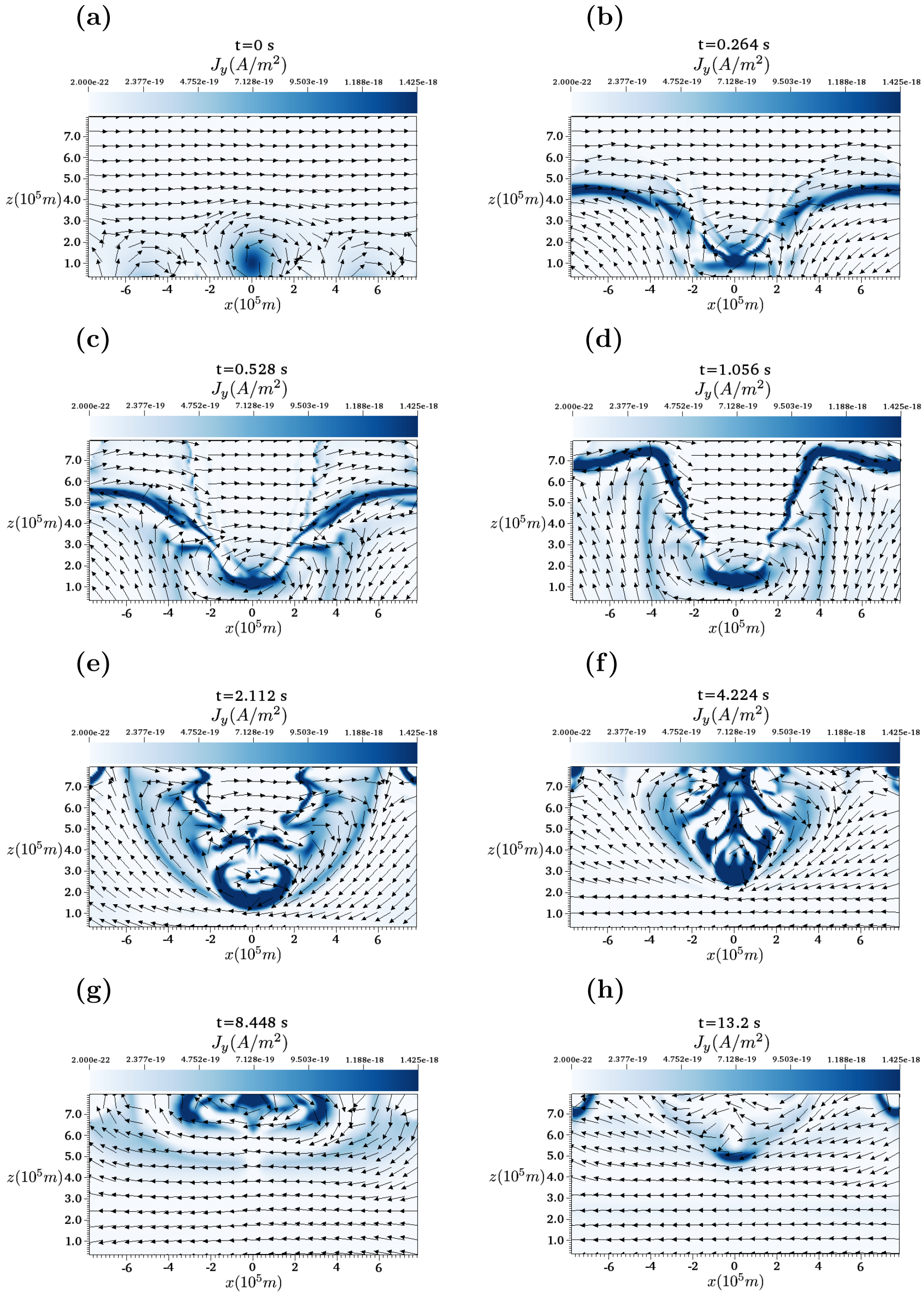

Figure 2. Snapshots of the evolution of the y-component of the current density $J_y(\mathrm{A/m^2})$ with the magnetic vector field for the case of the positive domain $z > 0$ at different times.

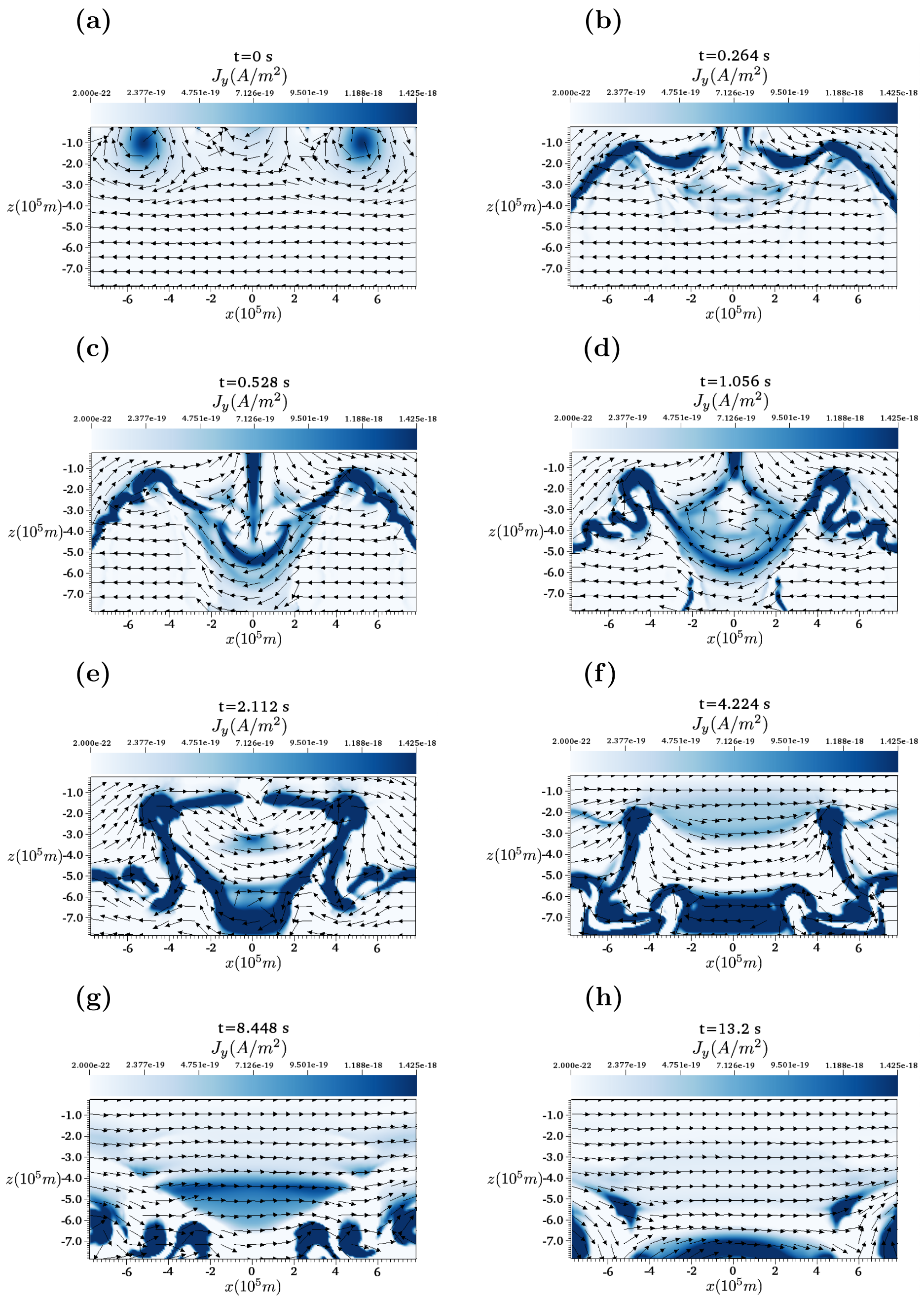

Figure 3. Snapshots of the evolution of the y-component of the current density $J_y(\mathrm{A/m^2})$ with magnetic vector field for the case of the negative domain $z < 0$ at different times.

magnetic island exactly at in the middle of the domain in the $x-$axis. In addition, we can identify two X-type neutral points at the top of the singularity. At times $t =$0.264 s and $t =$0.528 s, we can appreciate the fast evolution of the system, especially near the neutral points, which produce structures of high current density. At time t =1.056 s, we can see that the structures of the high current reach the top of the domain. At times $t =$2.112 s and $t =$4.224 s, we can identify the formation of a symmetric structure, which is caused by the evolution of the two X-type points. At time $t =$8.448 s, we can see that the structure practically disappears at the top of the domain. Finally, at time $t =$13.200 s, we can see that the polarity of the magnetic field is completely reversed, which may be due to the evolution of the two X-type neutral points.

For the second part of the domain ($z < 0$), we perform the simulation with ii) that we cover with 200×100 cells. We also use a constant Courant factor CFL=0.001 and impose open boundary conditions in all sides.

The results of this case are shown in Figure 3. For example, at the initial time, we can see two magnetic islands and X-type neutral points at the bottom of the singular points. At times t =0.264 s and t =0.528 s, we can see the fast evolution of the system, especially near the neutral points, which produce two structures of high current density that extended up to the middle of the domain. At time $t =$1.056 s, we can see that the two high current structures show fluctuations. At time $t =$2.112 s, we identify a high current structure that reaches the bottom of the domain. In addition, we notice the prevalence of the two initial high current structures forming a symmetric configuration near the initial position of the X-type points. In addition, at this time, we can observe that the polarity of the magnetic field starts to invert. At time $t =$4.224 s, we can see that the previous structure begins to dissipate. Finally, at the times $t =$8.448 s and $t =$13.200 s, the high current structures reach the bottom of the domain. In addition, in the same way as in the previous case, we can also observe that the polarity of the magnetic field was completely reversed.

7 Discussion

The specific form of the GS equation and its solutionphysically represents a magnetostatic problem. This could lead to the idea that the solution would be in magnetostatic equilibrium when set to evolve in a numerical and dynamic environment. Figures 2b and 3b, however, show very fast dissipation in less than one second of the magnetic islands of the initial configuration. Almost all structures left the integration region at 13.200 s. In addition, the magnetic field vector reverses its polarity very quickly. Consequently, if this structure exists in a real physical system, we barely have enough data to observe its evolution.

At the initial configuration, the structure found in the magnetic island is probably the signature of a twisted flux tube (Dasso et al., 2005; Démoulin & Dasso, 2009). Therefore, the model shows a fast way of transforming a flux-rope into an elongated current sheet, and the latter is the only structure, specifically a sample of it, which could be locally observed in any real physical system throughout its temporal evolution. By definition, a two-dimensional current sheet is related to a tangential discontinuity at a non-propagating boundary between two plasmas (Parnell, 2000). Current sheets have been found in the solar atmosphere, in the interplanetary medium, in the magnetosphere, as well as in comets (Yoon & Lui, 2005).

What makes this model important is the spatial location of the X-type neutral points, magnetic islands and singular points, respectively. The initial configuration is important because as shown in Figure 1c, the currents are well concentrated on the three magnetic islands, the two singular points are on the line $z = 0$, and the four X-type neutral points are localized between the islands and the singular points, far from the x-axis. Similarly

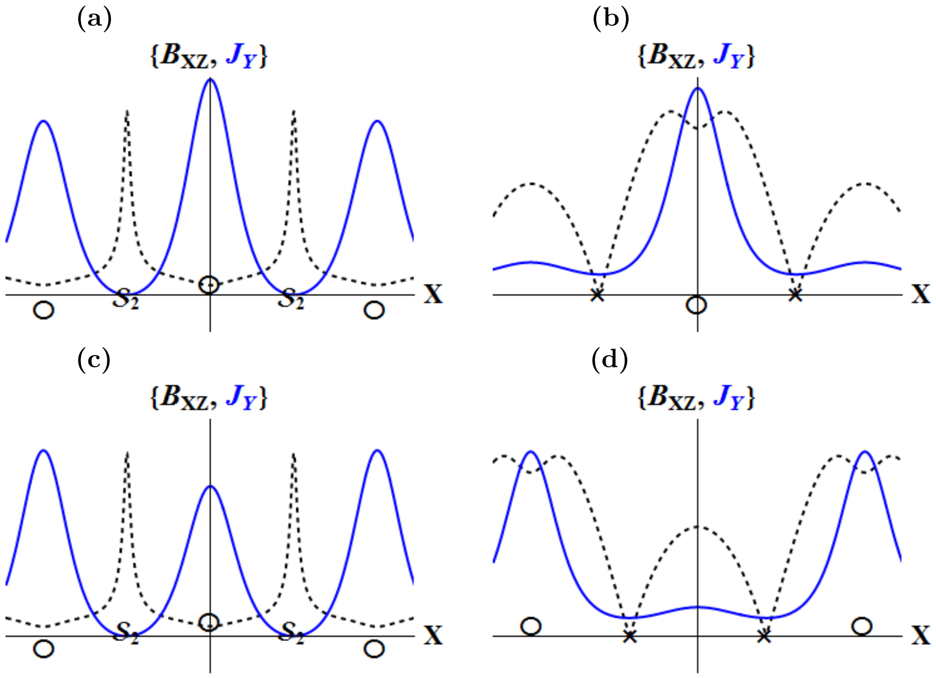

Figure 4. The physical behavior of the magnetic field (black dashed lines) and the current density (blue thin lines). Their respective point types (X- O- and S-types) are also shown.The left panels (a and c) correspond to the solutions behaviors for $z = \pm 0.1$ and the right panels (b and d) for $z = \pm 1.8$.

to Fadeev's model (Figure 1a), this configuration will be repeated periodically from minus infinity to plus infinity on the x-axis.

Fadeev's model in an MHD simulation shows that initially the only place where particles could diffuse is the X-type point through magnetic reconnection (Makwana et al., 2018). On the other hand, excluding the x-axis from our model, in each region ($z < 0$ and $z > 0$) there are two X-points instead of one. The aforementioned is one of the first facts that helps us to understand why our model is evolving so rapidly in the MHD environment because in a diffusion process two X-points are more efficient than one.

A second fact that helps us to understand the rapid evolution of the model is the magnetic field near the singular points. Figure 4 shows a schematic representation of the magnetic field magnitude (black dashed lines) and current density (blue thin lines) after making four horizontal cuts in Figure 1c as follows: (a) $z = 0.1$; (b) $z = 0.8$; (c) $z = -0.1$; and (d) $z = -0.8$. The location of each point type (X-, O-, and S-types) is also shown. All panels show the maximum of J_y at 0-type points and the null magnetic field at X-type points. Panels (a) and (c) show two amplitude peaks of the magnetic field near the singular points. The Figure 1c shows that the direction of the magnetic field within the islands is clockwise, while within the singular points the direction is the opposite. Therefore, this field will force a rapid evolution of the system to the opposite boundary. The interaction with the initially opposite field will force the creation of an elongated current sheet. Panels (b) and (d) show two X-points each. The two X-points on panel (d) are closer to the origin than the X-points on panel (b). Panel (b) shows the presence of a magnetic island, while panel (d) shows two.

In summary, the direction and amplitude of the magnetic field near the singular points and the existence of the X-points are the main cause forcing the model to have a fast diffusion. The magnetic islands disappear quickly, forming elongated current sheets that will leave the integration grid domain.

8 Summary and Conclusions

In this work, we introduce a new solution of the special form of the Grad-Shafranov equation (Grad & Rubin, 1958; Shafranov, 1966) using a combination of Fadeev (Fadeev et al., 1965) and NAVAL solutions (Laurindo-Sousa et al., 2018). The proposed solution defined in (17) shows singularity points where the cosine is zero. In particular, the two singular points are on the $z = 0$ and the four X-type neutral points are in between the islands and the singular points. The solutions are repeated periodically from minus infinity to plus infinity on the x-axis.

In addition, we used an MHD code (Newtonian CAFE) to study the time evolution of the proposed solution. We use the equation (17) to construct the initial conditions for a 2D MHD domain with open boundaries. The results of numerical simulations indicate that the evolution of the proposed solution shows increases in current density near the X-type points. An interesting property of the system is that it reverses the polarity of the magnetic field, which may be due to the direction as well as amplitude peaks of the magnetic field near the singular points, and the presence of X-type neutral points.

The main results of this article can be summarized as bellow.
(i) The generating functions of Fadeev and NAVAL have been grouped in a new way to obtain another solution given by (17).

(ii) The characteristics of the new solution have been described in detail, such as the location and the importance of the X-, O- and S-types points.

(iii) The singular points of the new solution have been excluded from the integration grid domain to perform an MHD simulation of the dynamic evolution of the initial condition defined in terms of (17).

(iv) In the MHD simulation it has been possible to observe the fast evolution of magnetic islands into current sheets;

(v) The importance of the strong magnetic field at the edge of the singular points has also been explained for understanding the polarity inversion and the fast evolution of the model.

(vi) As a limitation linked to the magnetic morphology of the new solution in a numeric and dynamic environment, the difficulty in finding a real physical system because of its fast temporal evolution is considered.

Acknowledgments

L. Nunes dos Santos thanks PROSUC-CAPES for the PhD scholarship in the Physics and Astronomy course at UNIVAP. A. Ojeda-González wishes to thank CNPq for financial support (grant 431396/2018-3). J. J. González-Avilés thanks to Cátedras CONACyT (CONACyT Fellow) for supporting this work. V. De la Luz thanks to CONACyT for financial support (grant Ciencia Básica 254497).

References

Ambrosino, G., & Albanese, R. (2005, 11). Magnetic control of plasma current, position, and shape in tokamaks - a survey of modeling and control approaches. *Control Systems, IEEE*, *25*, 76-92. doi: 10.1109/MCS.2005.1512797

Arzner, K., & Scholer, M. (2001, Mar). Kinetic structure of the post plasmoid plasma sheet during magnetotail reconnection. *J. Geophys. Res.*, *106*(A3), 3827-3844. doi: 10.1029/2000JA000179

Atanasiu, C. V., Günter, S., Lackner, K., & Miron, I. G. (2004, Jul). Analytical solutions to the Grad-Shafranov equation. *Physics of Plasmas*, *11*(7), 3510-3518.

doi: 10.1063/1.1756167

Becker, U., Neukirch, T., & Schindler, K. (2001, Mar). On the quasistatic development of thin current sheets in magnetotail-like magnetic fields. *J. Geophys. Res.*, *106*(A3), 3811-3826. doi: 10.1029/2000JA900141

Birn, J., & Hesse, M. (2001, Mar). Geospace Environment Modeling (GEM) magnetic reconnection challenge: Resistive tearing, anisotropic pressure and hall effects. *J. Geophys. Res.*, *106*(A3), 3737-3750. doi: 10.1029/1999JA001001

Biskamp, D. (1986, May). Magnetic reconnection via current sheets. *Physics of Fluids*, *29*, 1520-1531. doi: 10.1063/1.865670

Crowdy, D. G. (1997). General solutions to the 2d liouville equation. *International Journal of Engineering Science*, *35*(2), 141 - 149. Retrieved from `http://www.sciencedirect.com/science/article/pii/S0020722596000808` doi: https://doi.org/10.1016/S0020-7225(96)00080-8

Dasso, S., Mandrini, C. H., Démoulin, P., Luoni, M. L., & Gulisano, A. M. (2005). Large scale MHD properties of interplanetary magnetic clouds. *Adv. Space Res.*, *35*, 711-724. doi: 10.1016/j.asr.2005.02.096

Dedner, A., Kemm, F., Kröner, D., Munz, C.-D., Schitzer, T., & Wesenberg, M. (2002, Jan). Hyperbolic divergence cleaning for the mhd equations. *J. Comnput. Phys.*, *175*, 645-673. doi: 10.1006/jcph.2001.6961

Démoulin, P., & Dasso, S. (2009, May). Causes and consequences of magnetic cloud expansion. *Astron. Astrophys.*, *498*, 551-566. doi: 10.1051/0004-6361/200810971

Einfeldt, B. (1988). On Godunov-type methods for gas dynamics. *SIAM J. Numer. Anal.,*, *25*, 294-318.

Fadeev, V., Kvabtskhava, I., & Komarov, N. (1965). Self-focusing of local plasma currents. *Nucl. Fusion*, *5*(202), 202-209. doi: 10.1088/0029-5515/5/3/003

Génot, V. (2005). Comment on “a class of exact two-dimensional kinetic current sheet equilibria” by peter h. yoon and anthony t. y. lui. *Journal of Geophysical Research: Space Physics*, *110*(A9). doi: 10.1029/2005JA011035

González-Avilés, J., & Guzmán, F. (2018). CAFE-Q: Code Design to Solve the Resistive MHD Equations With Thermal Conductivity. *IEEE Trans. Plasma Sci.*, *46*, 2378-2385. doi: 10.1109/TPS.2018.2796312

González-Avilés, J. J., Cruz-Osorio, A., Lora-Clavijo, F., & Guzmán, F. S. (2015). Newtonian CAFE: a new ideal MHD code to study the solar atmosphere. *Monthly Notices of the Royal Astronomical Society*, *454*, 1871-1885. doi: 10.1093/mnras/stv2013

González-Avilés, J. J., & Guzmán, F. S. (2015). Estimating the contribution of Alfvén waves to the process of heating the quiet solar corona. *Monthly Notices of the Royal Astronomical Society*, *451*, 4819-4830. doi: 10.1093/mnras/stv959

Grad, H., & Rubin, H. (1958, Jan). Hydromagnetic Equilibria and Force-Free Fields. In *Proceedings of the 2nd un conference on the peaceful uses of atomic energy* (Vol. 31, pp. 190–197). Geneva: United Nations: United Nations.

Harris, E. G. (1962). On a plasma sheath separating regions of oppositely directed magnetic field. *Il Nuovo Cimento*, *23*(1), 115–121. doi: 10.1007/BF02733547

Harten, P., Engquist, B., Osher, S., & Chakravarthy, S. (1997, February). Uniformly High Order Accurate Essentially Non-oscillatory Schemes, III. *J. Comput. Phys.,*, *131*, 3-47. doi: https://doi.org/10.1006/jcph.1996.5632

Harten, P., Lax, P., & Van Leer, B. (1983). On Upstream Difference and Godunov-Type Schemes for Hyperbolic Conservation Laws. *SIAM Review*, *25*, 35-61. doi: https://doi.org/10.1137/1025002

Hau, L. N., & Sonnerup, B. U. Ö. (1999, Apr). Two-dimensional coherent structures in the magnetopause: Recovery of static equilibria from single-spacecraft data. *J. Geophys. Res.*, *104*(A4), 6899-6918. doi: 10.1029/1999JA900002

Hesse, M., Birn, J., & Kuznetsova, M. (2001, Mar). Collisionless magnetic reconnection: Electron processes and transport modeling. *J. Geophys. Res.*, *106*(A3), 3721-3736. doi: 10.1029/1999JA001002

Hu, Q. (2017, Aug 01). The grad-shafranov reconstruction in twenty years: 1996–2016. *Science China Earth Sciences*, *60*(8), 1466–1494. Retrieved from https://doi.org/10.1007/s11430-017-9067-2 doi: 10.1007/s11430-017-9067-2

Hu, Q., Smith, C. W., Ness, N. F., & Skoug, R. M. (2004, March). Multiple flux rope magnetic ejecta in the solar wind. *Journal of Geophysical Research (Space Physics)*, *109*(A18), 3102. doi: 10.1029/2003JA010101

Hu, Q., & Sonnerup, B. U. Ö. (2001). Reconstruction of magnetic flux ropes in the solar wind. *Geophysical Research Letters*, *28*(3), 467-470. Retrieved from https://agupubs.onlinelibrary.wiley.com/doi/abs/10.1029/2000GL012232 doi: 10.1029/2000GL012232

Kan, J. R. (1973). On the structure of the magnetotail current sheet. *Journal of Geophysical Research*, *78*(19), 3773–3781. Retrieved from http://dx.doi.org/10.1029/JA078i019p03773 doi: 10.1029/JA078i019p03773

Kan, J. R. (1979, Apr). Non-linear tearing structures in equilibrium current sheet. *Planet. Space Sci.*, *27*(4), 351-354. doi: 10.1016/0032-0633(79)90112-0

Korovinskiy, D. B., Kubyshkina, D. I., Semenov, V. S., Kubyshkina, M. V., Erkaev, N. V., & Kiehas, S. A. (2018). On application of asymmetric kan-like exact equilibria to the earth magnetotail modeling. *Ann. Geophys.*, *36*(2), 641–653. Retrieved from https://www.ann-geophys.net/36/641/2018/ doi: 10.5194/angeo-36-641-2018

Kuznetsova, M. M., Hesse, M., & Winske, D. (2001, Mar). Collisionless reconnection supported by nongyrotropic pressure effects in hybrid and particle simulations. *J. Geophys. Res.*, *106*(A3), 3799-3810. doi: 10.1029/1999JA001003

Lackner, K. (1976, Jan). Computation of ideal MHD equilibria. *Comput. Phys. Comm.*, *12*, 33. doi: https://doi.org/10.1016/0010-4655(76)90008-4

Laurindo-Sousa, A. N., Ojeda-González, A., Prestes, A., Klausner, V., & Caritá, L. A. (2018, Feb 01). New analytical solution of the equilibrium ampere's law using the walker's method: a didactic example. *Brazilian Journal of Physics*, *48*(1), 67–73. Retrieved from https://doi.org/10.1007/s13538-017-0542-8 doi: 10.1007/s13538-017-0542-8

Lui, A. T. Y., Sibeck, D. G., Phan, T., Angelopoulos, V., McFadden, J., Carlson, C., ... Frey, S. (2008, April). Reconstruction of a magnetic flux rope from THEMIS observations. *Geophysical Research Letters*, *351*, 17. doi: 10.1029/2007GL032933

Ma, Z. W., & Bhattacharjee, A. (2001, Mar). Hall magnetohydrodynamic reconnection: The Geospace Environment Modeling challenge. *J. Geophys. Res.*, *106*(A3), 3773-3782. doi: 10.1029/1999JA001004

Makwana, K., Keppens, R., & Lapenta, G. (2018, may). Two-way coupled MHD-PIC simulations of magnetic reconnection in magnetic island coalescence. *Journal of Physics: Conference Series*, *1031*, 012019. Retrieved from https://doi.org/10.1088%2F1742-6596%2F1031%2F1%2F012019 doi: 10.1088/1742-6596/1031/1/012019

Manankova, A., Pudovkin, M., & Runov, A. (2000). Stationary configurations of the two-dimensional current-carrying plasma sheet: Exact solutions. *Geomagn. Aeron.*, *40*, 430-438.

Manankova, A. V. (2003, December). Two-dimensional current-carrying plasma sheet in the near-Earth geomagnetic tail region: a quasi-stationary evolution. *Ann. Geophys.*, *21*, 2259-2269. doi: 10.5194/angeo-21-2259-2003

Manankova, A. V., & Pudovkin, M. I. (1996). Energy Characteristics of a Two-Dimensional Current-Carrying Plasma. *Geomagn. Aeron.*, *39*, 426-431.

Manankova, A. V., & Pudovkin, M. I. (1999). The description of a two-dimensional current-carrying plasma sheet in the hydrodynamic approximation of a single-

component plasma model. *Geomagn. Aeron.*, *39*, 40-44.
Mc Carthy, P. J. (1999, Sep). Analytical solutions to the Grad-Shafranov equation for tokamak equilibrium with dissimilar source functions. *Physics of Plasmas*, *6*(9), 3554-3560. doi: 10.1063/1.873630
Ojeda-González, A., Domingues, M. O., Mendes, O., Kaibara, M. K., & Prestes, A. (2015, Oct). Grad-Shafranov Reconstruction: Overview and Improvement of the Numerical Solution Used in Space Physics. *Brazilian Journal of Physics*, *45*(5), 493-509. doi: 10.1007/s13538-015-0342-y
Ojeda-González, A., Klausner, V., Mendes, O., Domingues, M. O., & Prestes, A. (2017a, nov). Characterization of the Complex Ejecta Measured In Situ on 19 – 22 March 2001 by Six Different Methods. *Solar Phys.*, *292*, 160. doi: 10.1007/s11207-017-1182-4
Ojeda-González, A., Prestes, A., & Laurindo Sousa, A. N. (2016, Aug). Discussion About the Magnetic Field Dimensionality, Invariant Axis Condition, and Coulomb Gauge to Solve the Grad-Shafranov Equation. *Brazilian Journal of Physics*, *46*(4), 408-414. doi: 10.1007/s13538-016-0422-7
Otto, A. (2001, Mar). Geospace Environment Modeling (GEM) magnetic reconnection challenge: MHD and Hall MHD-constant and current dependent resistivity models. *J. Geophys. Res.*, *106*(A3), 3751-3758. doi: 10.1029/1999JA001005
Parnell, C. E. (2000). Magnetic Reconnection: Classical Aspects. In J. P. Rozelot, L. Klein, & J.-C. Vial (Eds.), *Transport and energy conversion in the heliosphere* (Vol. 553, p. 61).
Pritchett, P. L. (2001, Mar). Geospace Environment Modeling magnetic reconnection challenge: Simulations with a full particle electromagnetic code. *J. Geophys. Res.*, *106*(A3), 3783-3798. doi: 10.1029/1999JA001006
Schindler, K. (2006). *Physics of Space Plasma Activity.* Physics of Space Plasma Activity, by Karl Schindler, pp. 522. Cambridge University Press, November 2006. ISBN-10: 0521858976. ISBN-13: 9780521858977. doi: 10.2277/0521858976
Shafranov, V. D. (1966, Jan). Plasma Equilibrium in a Magnetic Field. *Reviews of Plasma Physics*, *2*(1), 103.
Shay, M. A., Drake, J. F., Rogers, B. N., & Denton, R. E. (2001, Mar). Alfvénic collisionless magnetic reconnection and the Hall term. *J. Geophys. Res.*, *106*(A3), 3759-3772. doi: 10.1029/1999JA001007
Sonnerup, B. U. Ö., & Guo, M. (1996). Magnetopause transects. *Geophysical Research Letters*, *23*, 3679-3682. Retrieved from `http://dx.doi.org/10.1029/96GL03573` doi: 10.1029/96GL03573
Sonnerup, B. U. Ö., Hasegawa, H., Teh, W.-L., & Hau, L.-N. (2006). Grad-shafranov reconstruction: An overview. *Journal of Geophysical Research: Space Physics*, *111*(A9). Retrieved from `https://agupubs.onlinelibrary.wiley.com/doi/abs/10.1029/2006JA011717` doi: 10.1029/2006JA011717
Stuart, J. T. (1967, Jan). On finite amplitude oscillations in laminar mixing layers. *Journal of Fluid Mechanics*, *29*, 417-440. doi: 10.1017/S0022112067000941
Teh, W.-L. (2018, Nov). Erratum: Correction to: Grad-Shafranov reconstruction of magnetohydrostatic equilibria with nonisotropic plasma pressure: the theory. *Earth, Planets, and Space*, *70*(1), 185. doi: 10.1186/s40623-018-0953-y
Tóth, G. (2000, July). The $\nabla \cdot \mathbf{b} = 0$ constraint in shock-capturing magnetohydrodynamics codes. *J. Comnput. Phys.*, *161*, 605-652. doi: 10.1006/jcph.2000.6519
Walker, G. W. (1915, July). Some Problems Illustrating the Forms of Nebulae. *Royal Society of London Proceedings Series A*, *91*, 410–420. Retrieved from `http://www.jstor.org/stable/93512` doi: 10.1098/rspa.1915.0032
Yoon, P. H., & Lui, A. T. Y. (2005, Jan). A class of exact two-dimensional kinetic current sheet equilibria. *Journal of Geophysical Research (Space Physics)*, *110*(A1), A01202. doi: 10.1029/2003JA010308

Yoon, P. H., & Lui, A. T. Y. (2005b). Reply to comment by v. génot on “a class of exact two-dimensional kinetic current sheet equilibria”. *Journal of Geophysical Research: Space Physics*, *110*(A9). doi: 10.1029/2005JA011104

Zheng, S. B., Wootton, A. J., & Solano, E. R. (1996, Mar). Analytical tokamak equilibrium for shaped plasmas. *Physics of Plasmas*, *3*, 1176-1178. doi: 10.1063/1.871772

Fig1a.

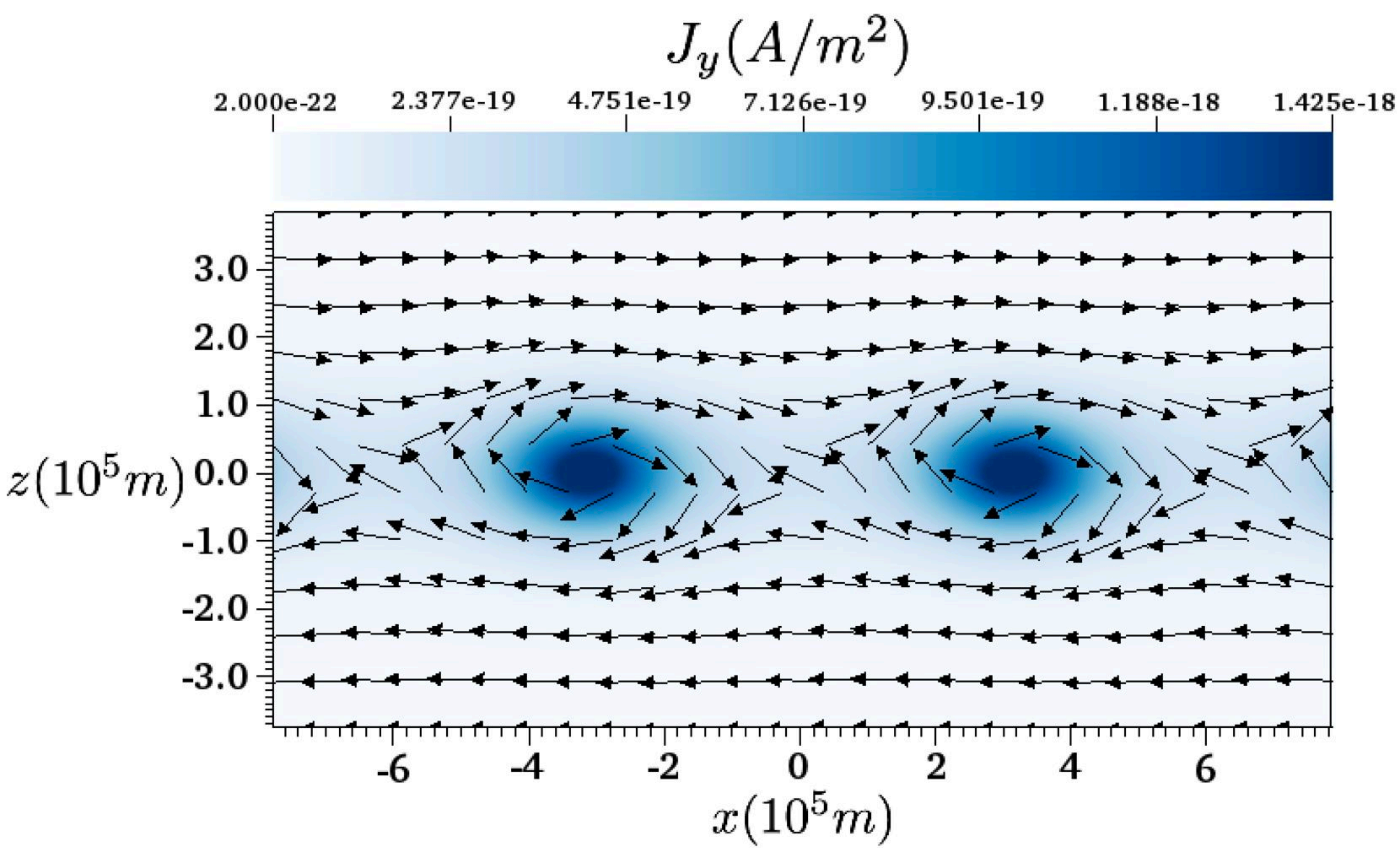
$J_y(A/m^2)$
2.000e-22
2.377e-19
4.751e-19
7.126e-19
9.501e-19
1.188e-18
1.425e-18
3.0
2.0
1.0
0.0
-1.0
-2.0
-3.0
$z(10^5m)$
-6
-4
-2
0
2
4
6
$x(10^5m)$

Fig1b.

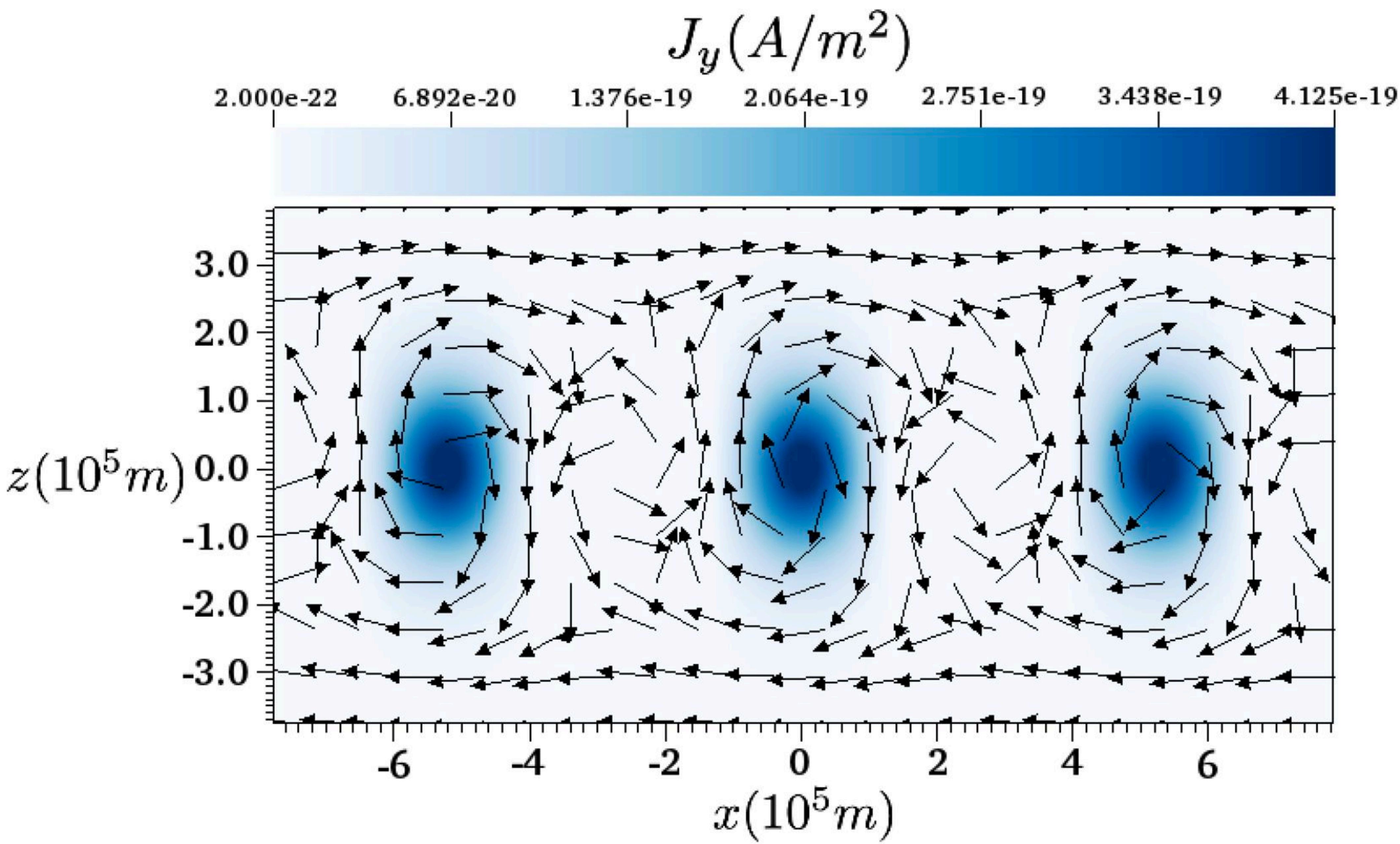

$J_y(A/m^2)$
2.000e-22
6.892e-20
1.376e-19
2.064e-19
2.751e-19
3.438e-19
4.125e-19
3.0
2.0
1.0
0.0
-1.0
-2.0
-3.0
$z(10^5 m)$
-6
-4
-2
0
2
4
6
$x(10^5 m)$

Fig1c.

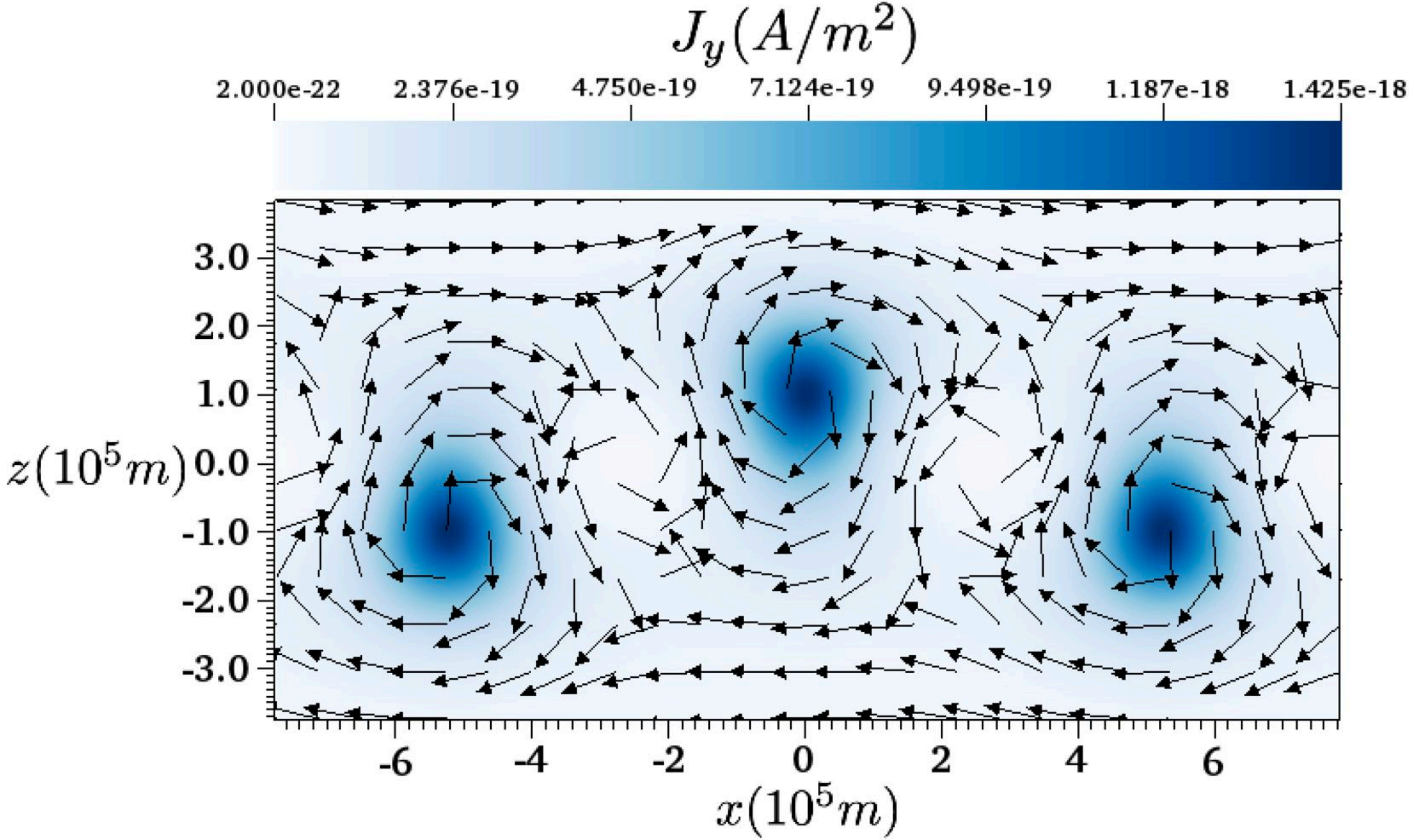

$J_y(A/m^2)$
2.000e-22
2.376e-19
4.750e-19
7.124e-19
9.498e-19
1.187e-18
1.425e-18
3.0
2.0
1.0
0.0
-1.0
-2.0
-3.0
$z(10^5m)$
-6
-4
-2
0
2
4
6
$x(10^5m)$

Fig2a.

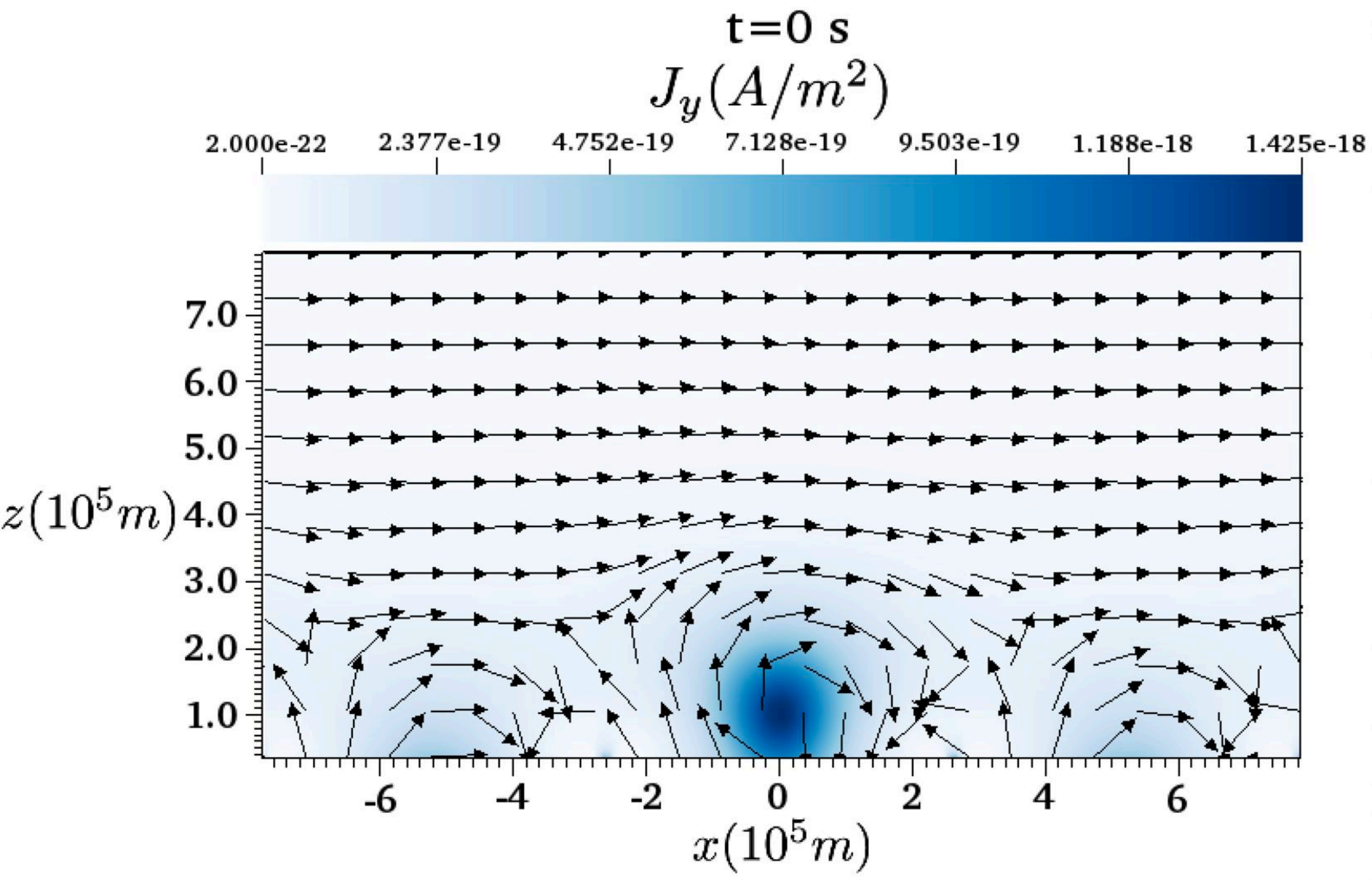
t=0 s
$J_y(A/m^2)$
2.000e-22
2.377e-19
4.752e-19
7.128e-19
9.503e-19
1.188e-18
1.425e-18
7.0
6.0
5.0
4.0
3.0
2.0
1.0
$z(10^5 m)$
-6
-4
-2
0
2
4
6
$x(10^5 m)$

Fig2b.

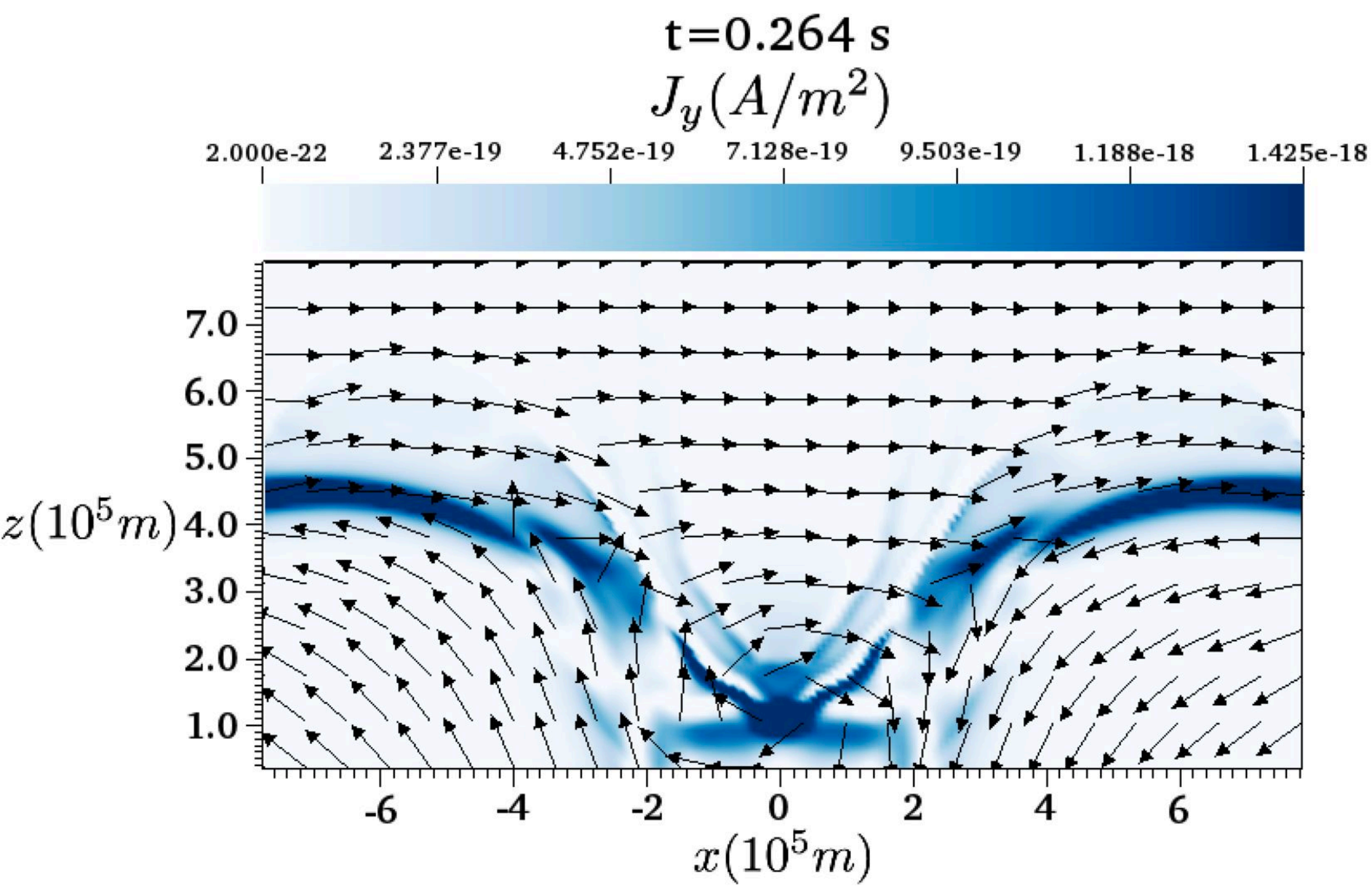

t=0.264 s
$J_y(A/m^2)$
2.000e-22
2.377e-19
4.752e-19
7.128e-19
9.503e-19
1.188e-18
1.425e-18
7.0
6.0
5.0
4.0
3.0
2.0
1.0
$z(10^5 m)$
-6
-4
-2
0
2
4
6
$x(10^5 m)$

Fig2c.

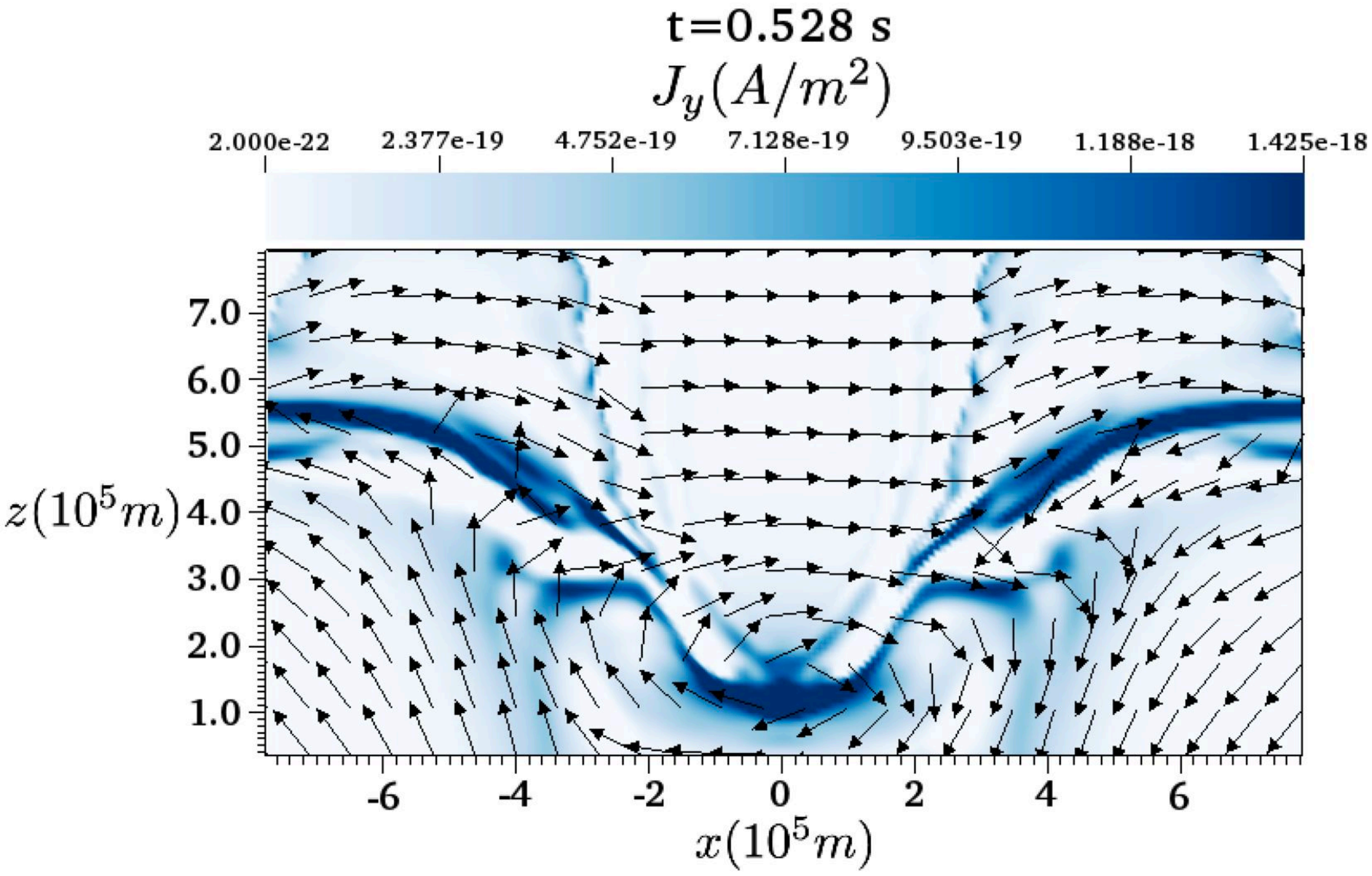

t=0.528 s
$J_y(A/m^2)$
2.000e-22
2.377e-19
4.752e-19
7.128e-19
9.503e-19
1.188e-18
1.425e-18
$z(10^5 m)$
7.0
6.0
5.0
4.0
3.0
2.0
1.0
-6
-4
-2
0
2
4
6
$x(10^5 m)$

Fig2d.

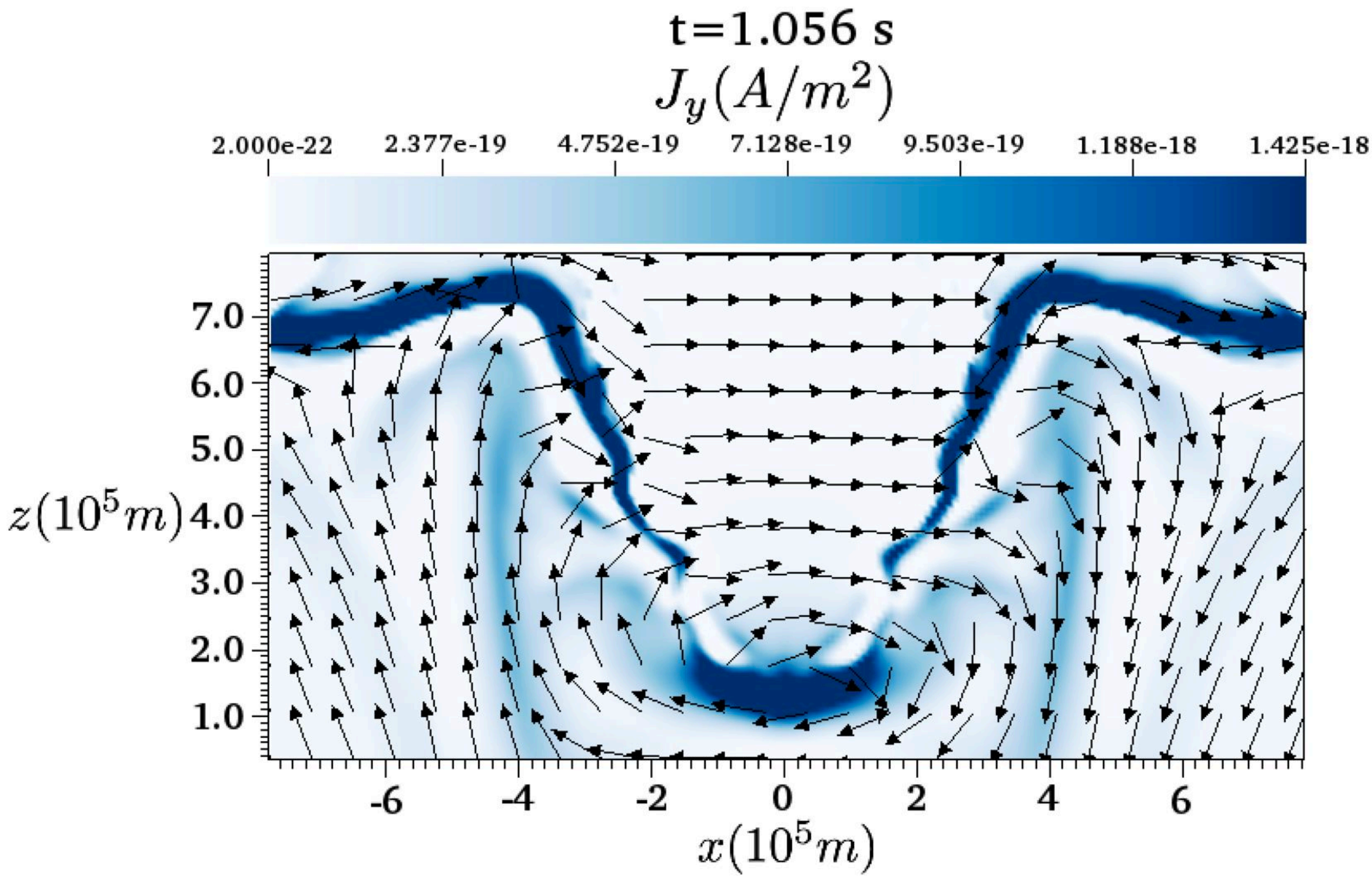

t=1.056 s
$J_y(A/m^2)$
2.000e-22
2.377e-19
4.752e-19
7.128e-19
9.503e-19
1.188e-18
1.425e-18
7.0
6.0
5.0
4.0
3.0
2.0
1.0
$z(10^5m)$
-6
-4
-2
0
2
4
6
$x(10^5m)$

Fig2e.

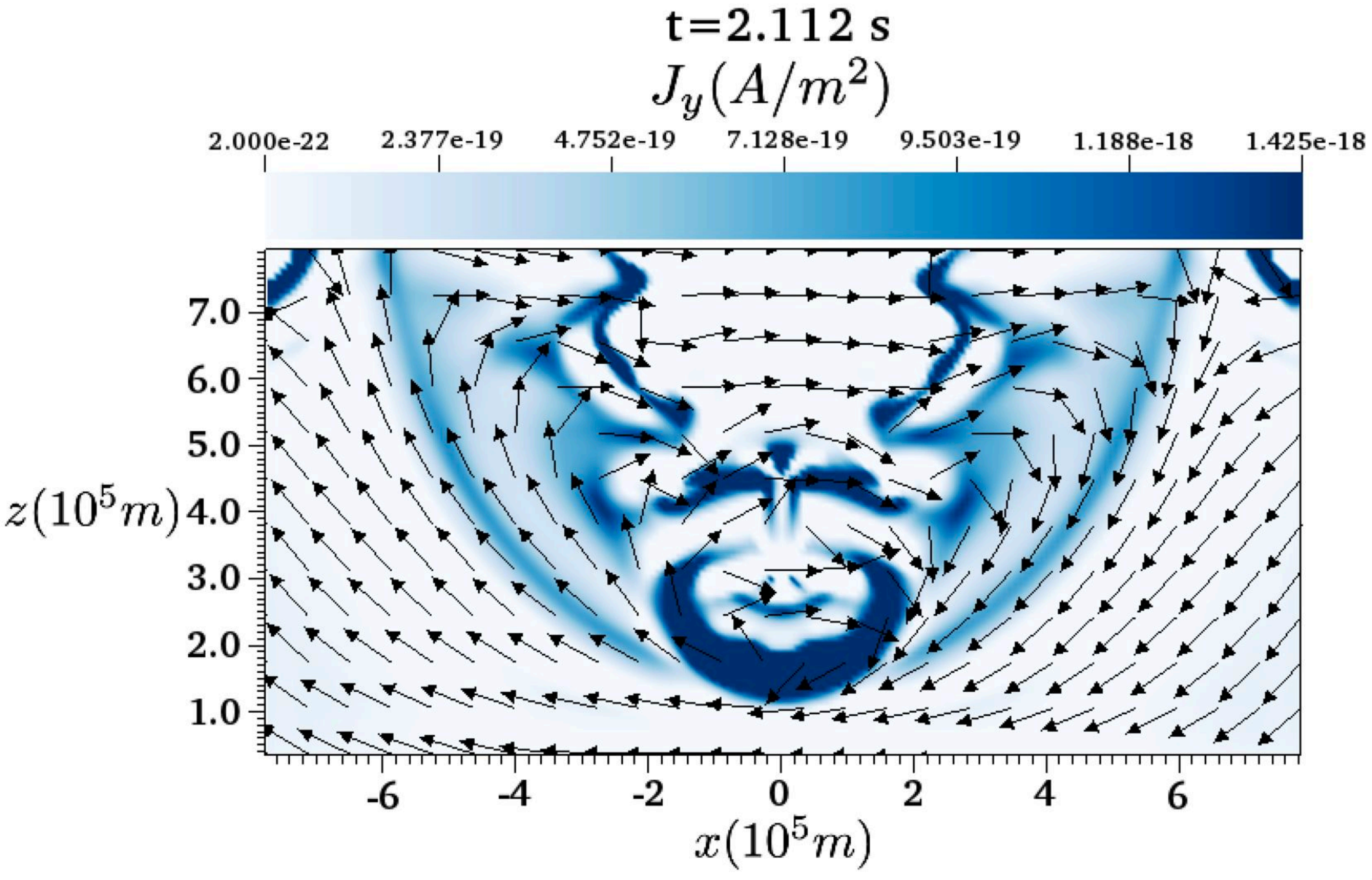

t=2.112 s
$J_y(A/m^2)$
2.000e-22
2.377e-19
4.752e-19
7.128e-19
9.503e-19
1.188e-18
1.425e-18
$z(10^5 m)$
7.0
6.0
5.0
4.0
3.0
2.0
1.0
-6
-4
-2
0
2
4
6
$x(10^5 m)$

Fig2f.

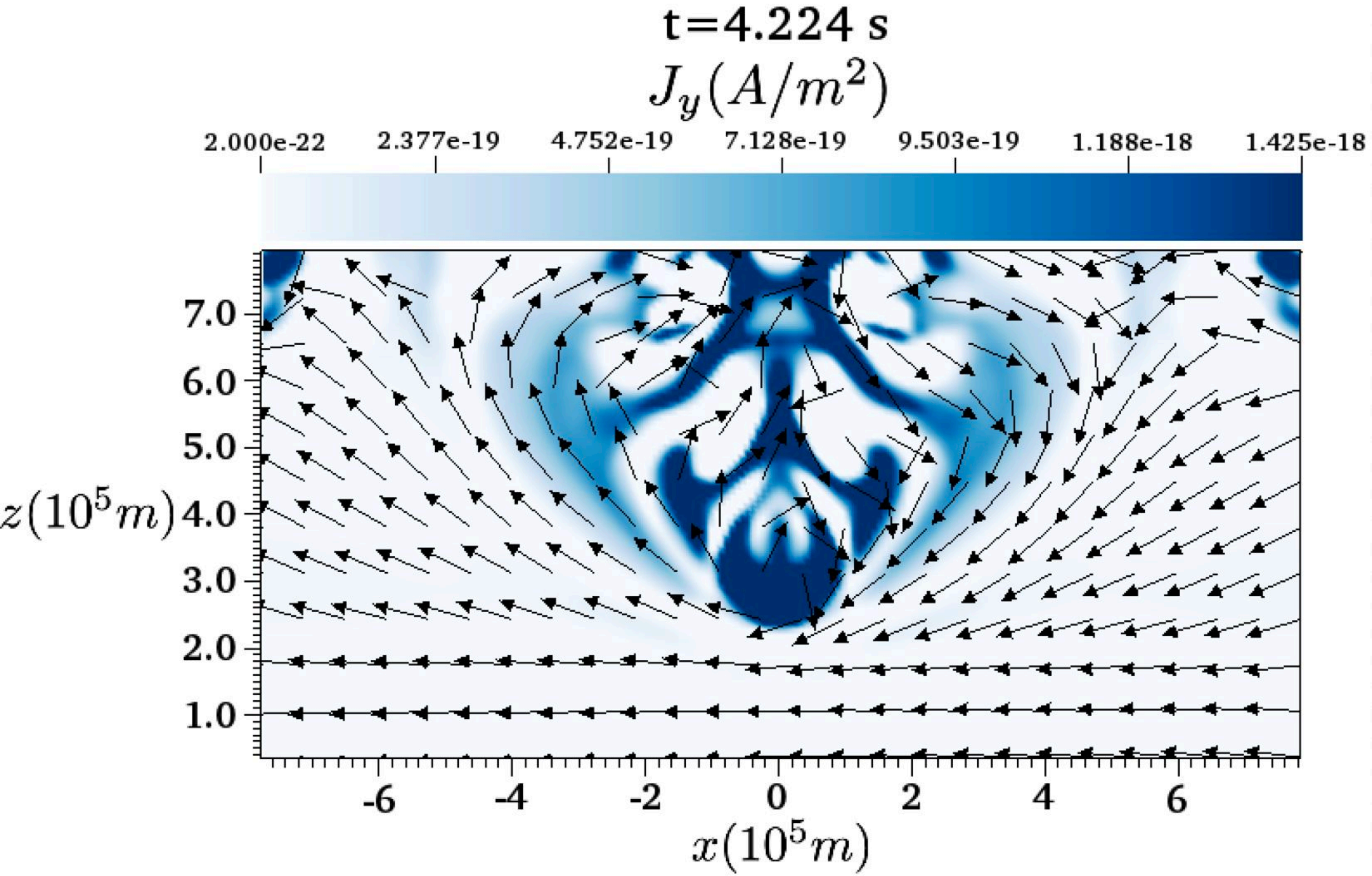

t=4.224 s
$J_y(A/m^2)$
2.000e-22
2.377e-19
4.752e-19
7.128e-19
9.503e-19
1.188e-18
1.425e-18
$z(10^5 m)$
7.0
6.0
5.0
4.0
3.0
2.0
1.0
-6
-4
-2
0
2
4
6
$x(10^5 m)$

Fig2g.

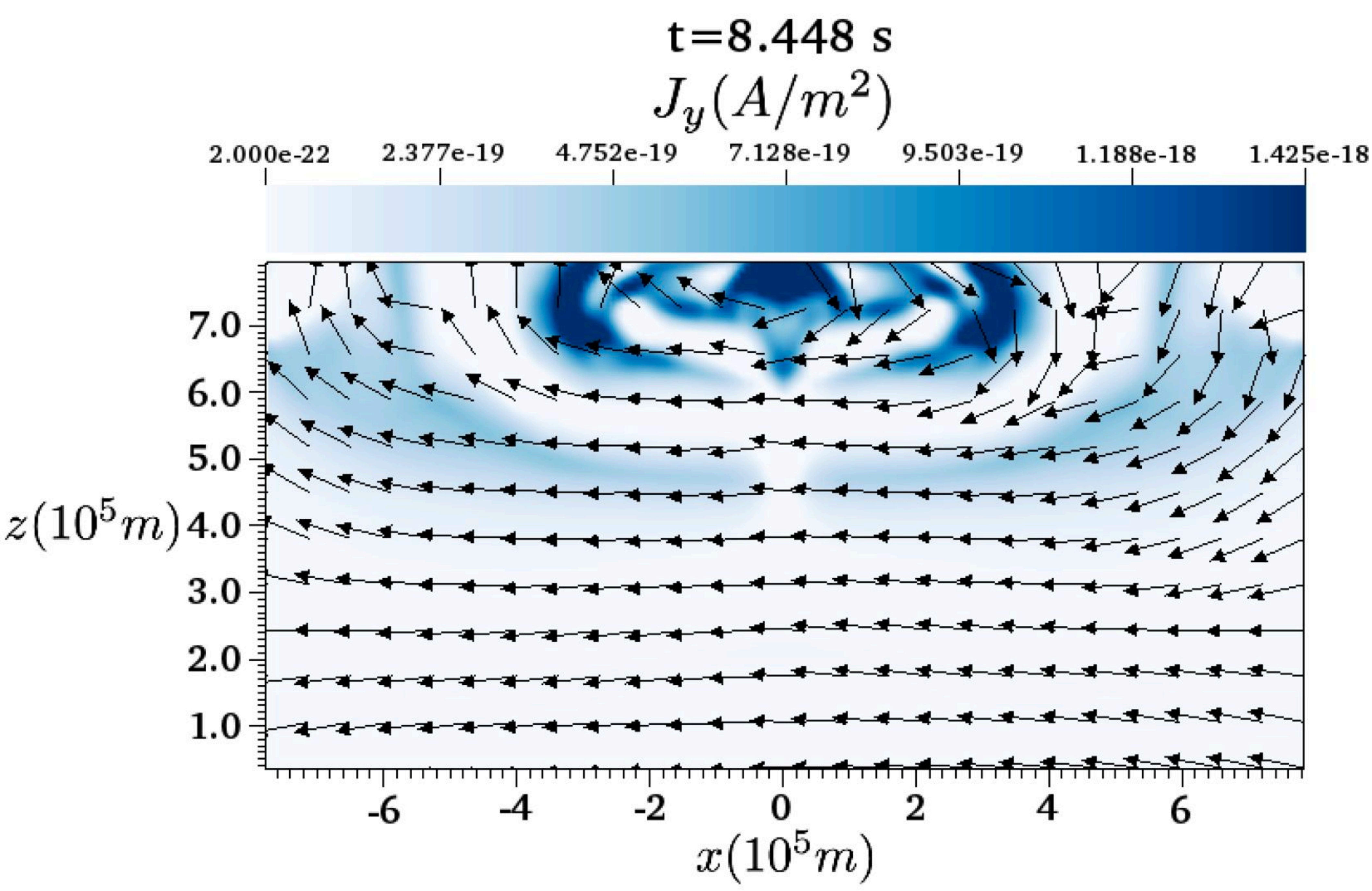

t=8.448 s
$J_y (A/m^2)$
2.000e-22
2.377e-19
4.752e-19
7.128e-19
9.503e-19
1.188e-18
1.425e-18
7.0
6.0
5.0
4.0
3.0
2.0
1.0
$z(10^5 m)$
-6
-4
-2
0
2
4
6
$x(10^5 m)$

Fig2h.

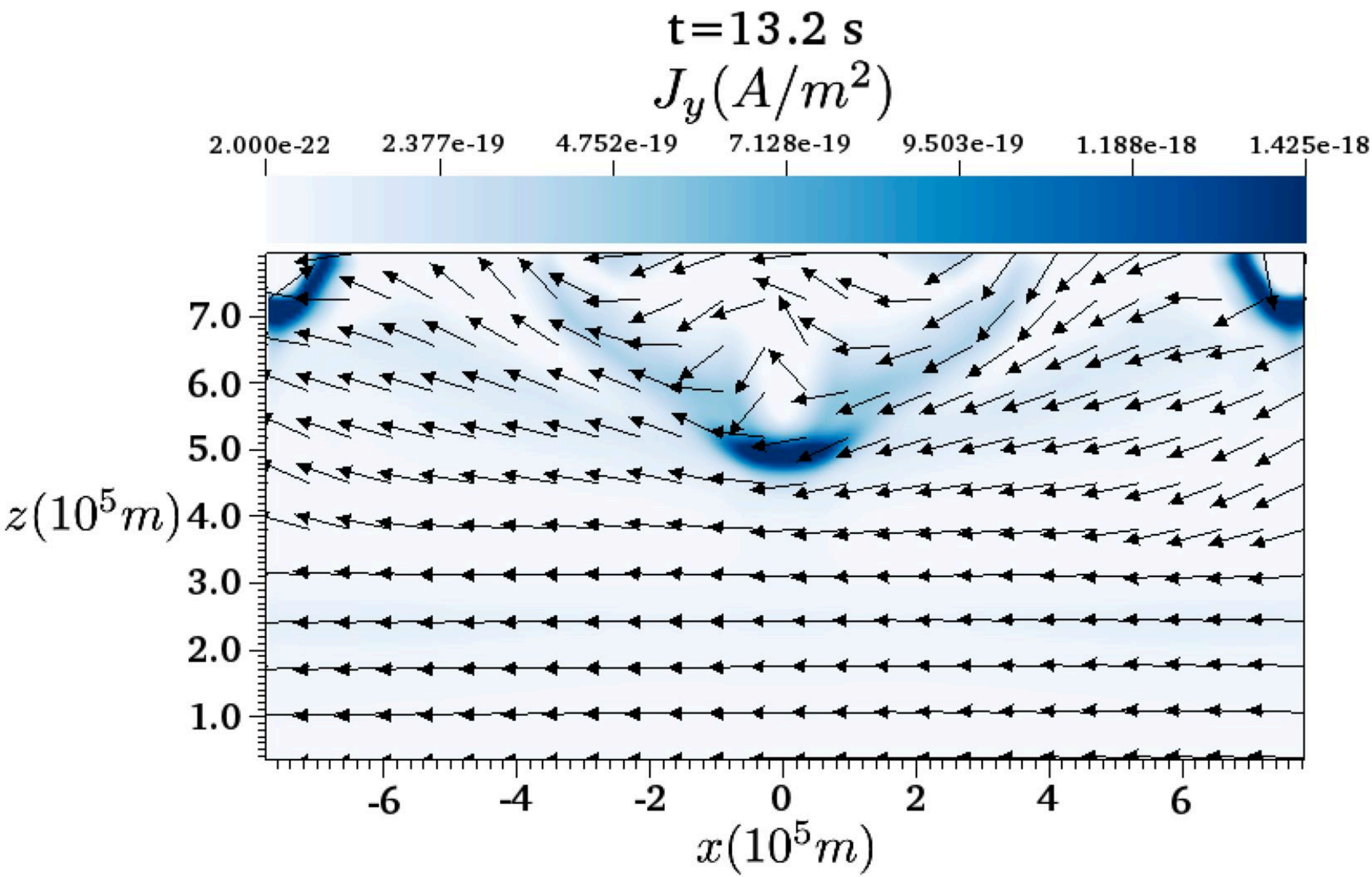

t=13.2 s
$J_y (A/m^2)$
2.000e-22
2.377e-19
4.752e-19
7.128e-19
9.503e-19
1.188e-18
1.425e-18
$z(10^5 m)$
7.0
6.0
5.0
4.0
3.0
2.0
1.0
-6
-4
-2
0
2
4
6
$x(10^5 m)$

Fig3a.

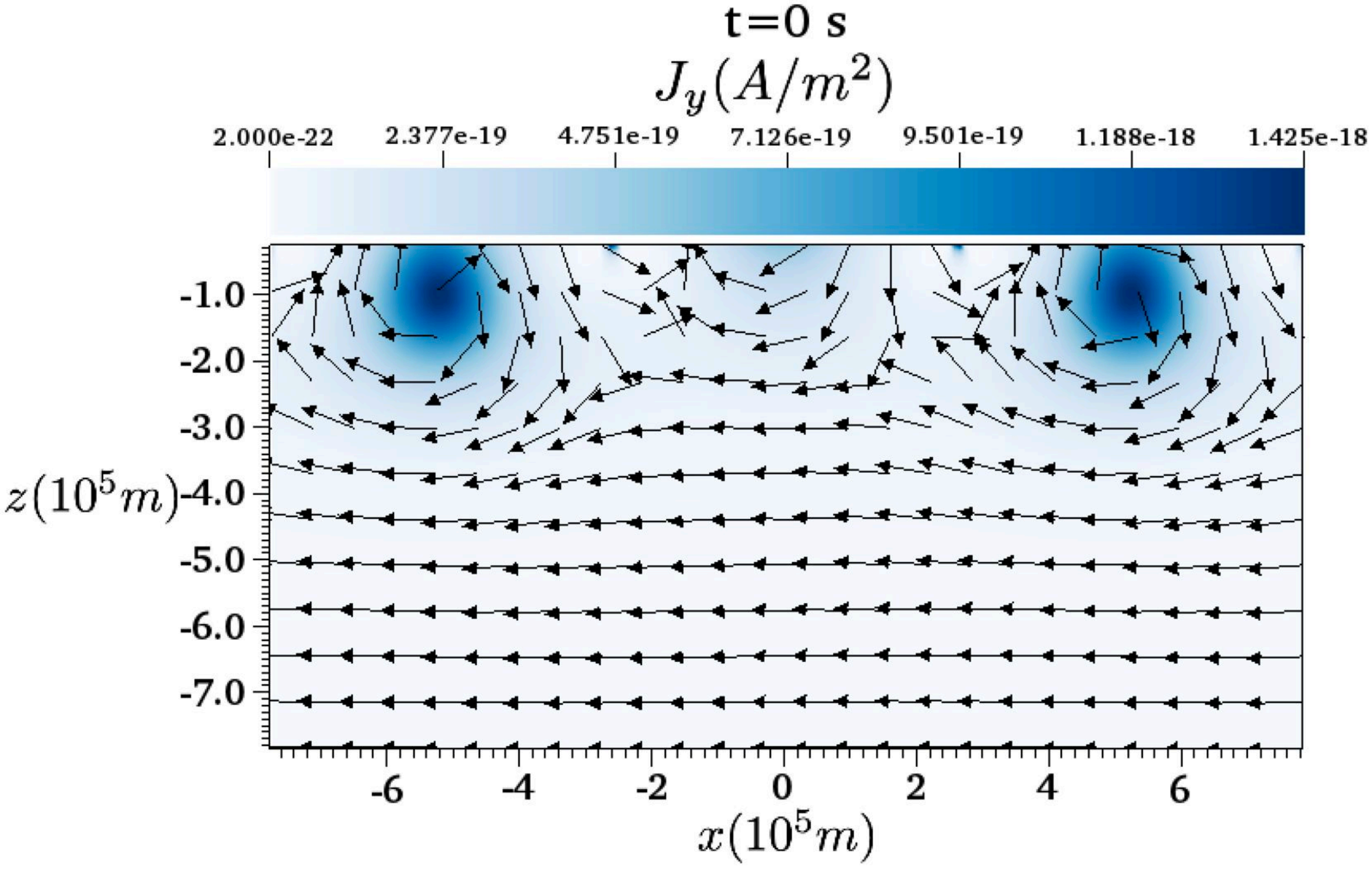

t=0 s
$J_y(A/m^2)$
2.000e-22
2.377e-19
4.751e-19
7.126e-19
9.501e-19
1.188e-18
1.425e-18
$z(10^5m)$
-1.0
-2.0
-3.0
-4.0
-5.0
-6.0
-7.0
$x(10^5m)$
-6
-4
-2
0
2
4
6

Fig3b.

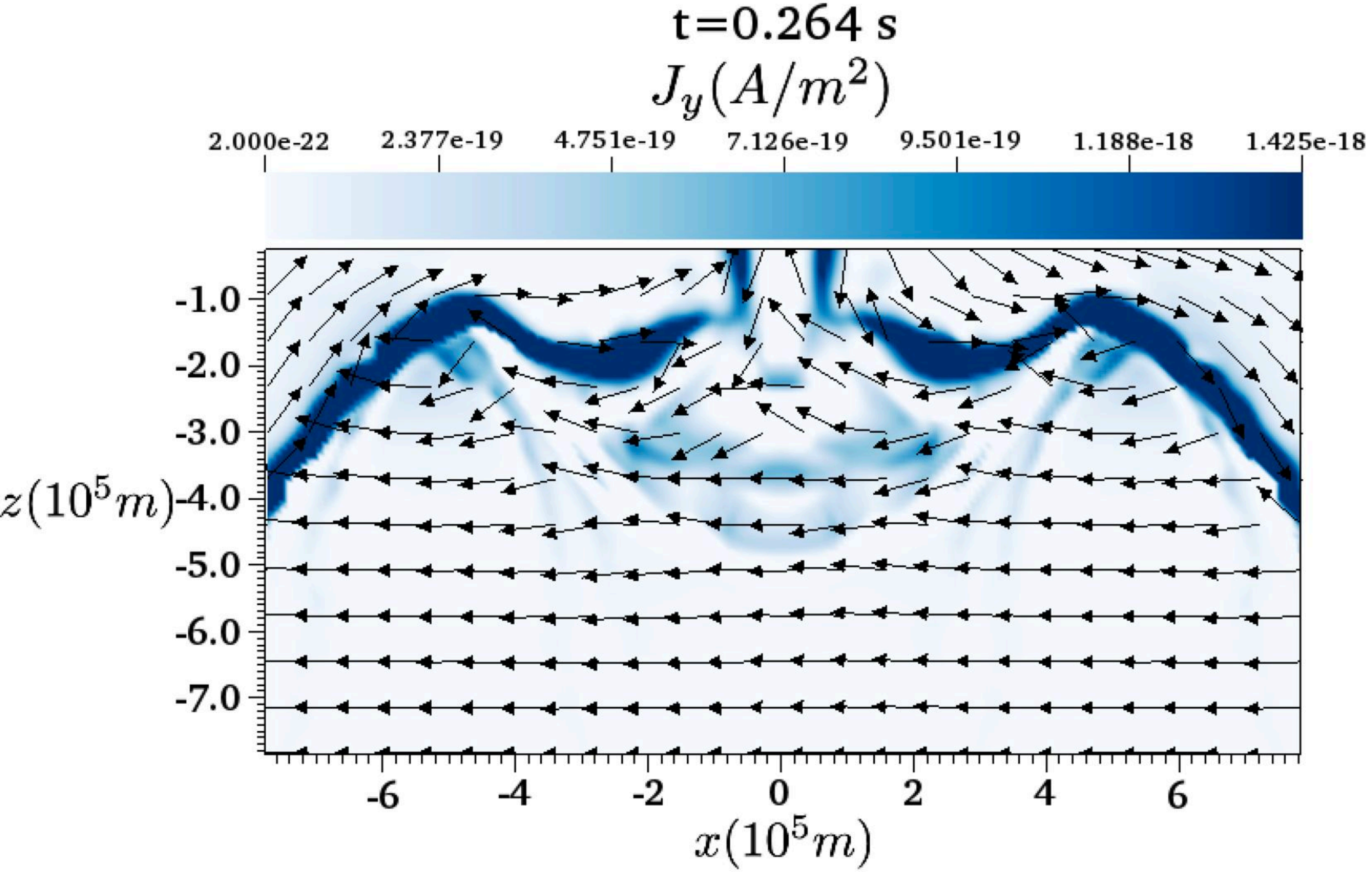

t=0.264 s
$J_y(A/m^2)$
2.000e-22
2.377e-19
4.751e-19
7.126e-19
9.501e-19
1.188e-18
1.425e-18
-1.0
-2.0
-3.0
$z(10^5m)$-4.0
-5.0
-6.0
-7.0
-6
-4
-2
0
2
4
6
$x(10^5m)$

Fig3c.

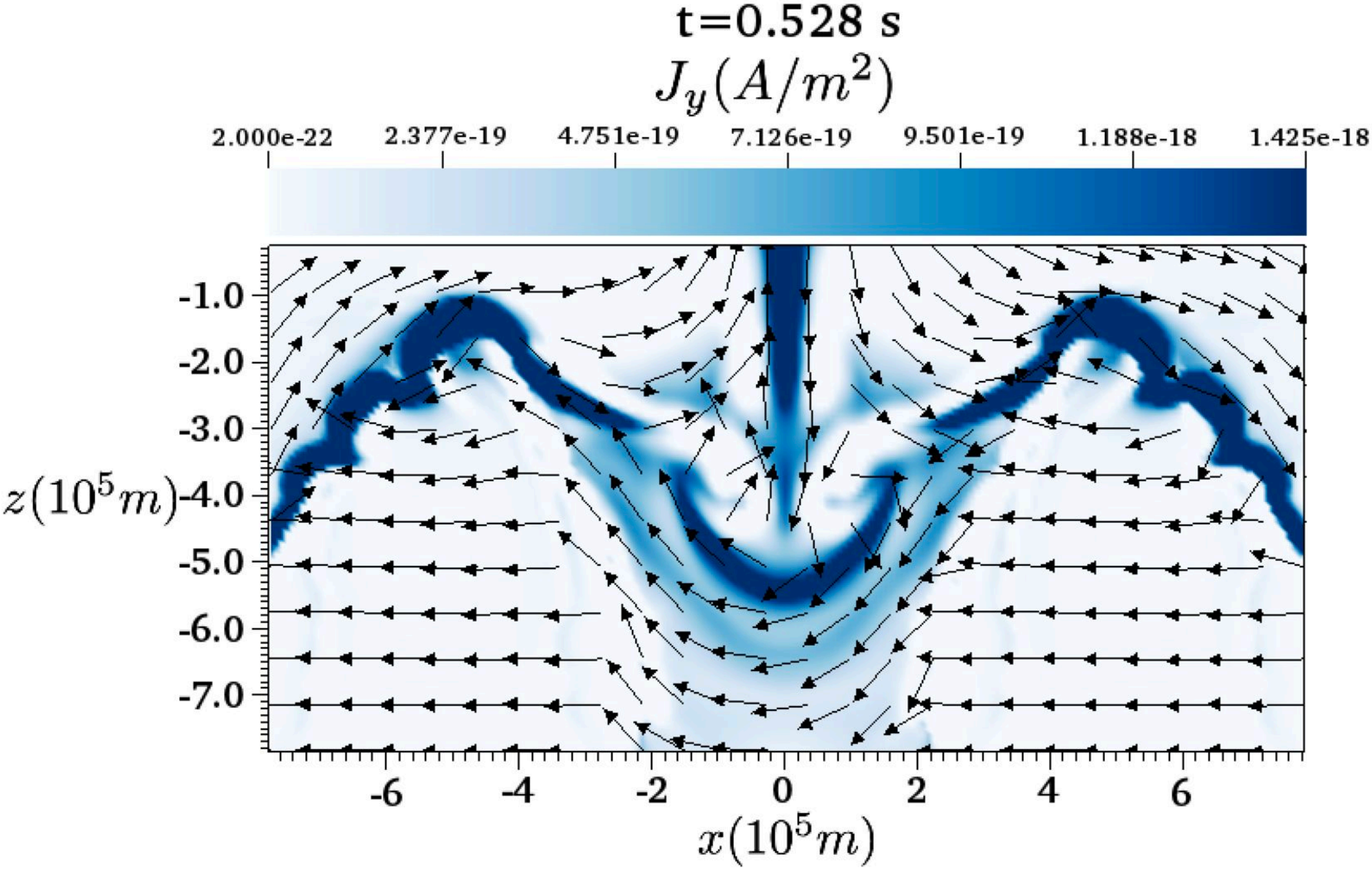
t=0.528 s
$J_y(A/m^2)$
2.000e-22
2.377e-19
4.751e-19
7.126e-19
9.501e-19
1.188e-18
1.425e-18
-1.0
-2.0
-3.0
$z(10^5m)$
-4.0
-5.0
-6.0
-7.0
-6
-4
-2
0
2
4
6
$x(10^5m)$

Fig3d.

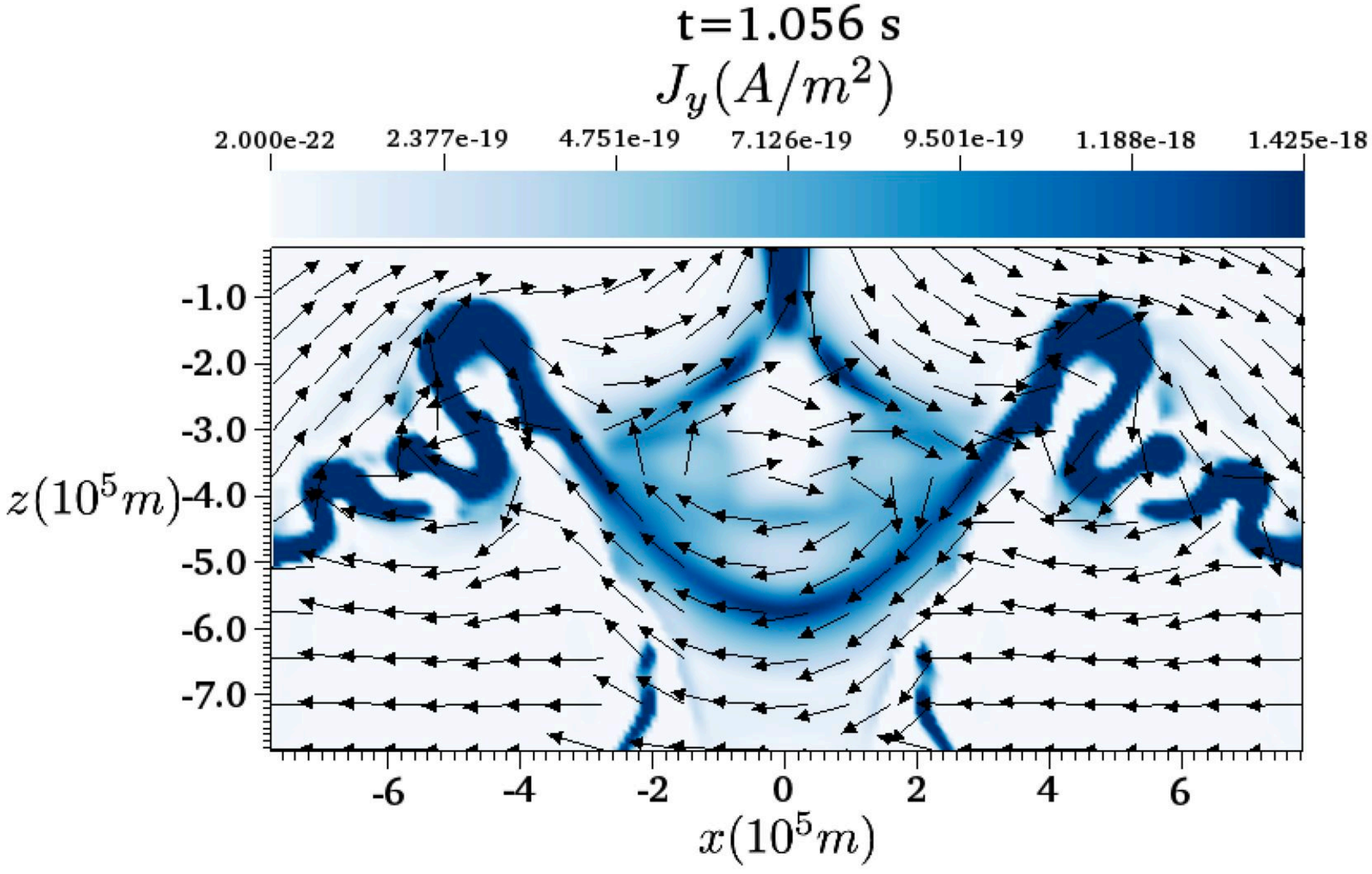
t=1.056 s
$J_y(A/m^2)$
2.000e-22
2.377e-19
4.751e-19
7.126e-19
9.501e-19
1.188e-18
1.425e-18
-1.0
-2.0
-3.0
-4.0
-5.0
-6.0
-7.0
$z(10^5m)$
-6
-4
-2
0
2
4
6
$x(10^5m)$

Fig3e.

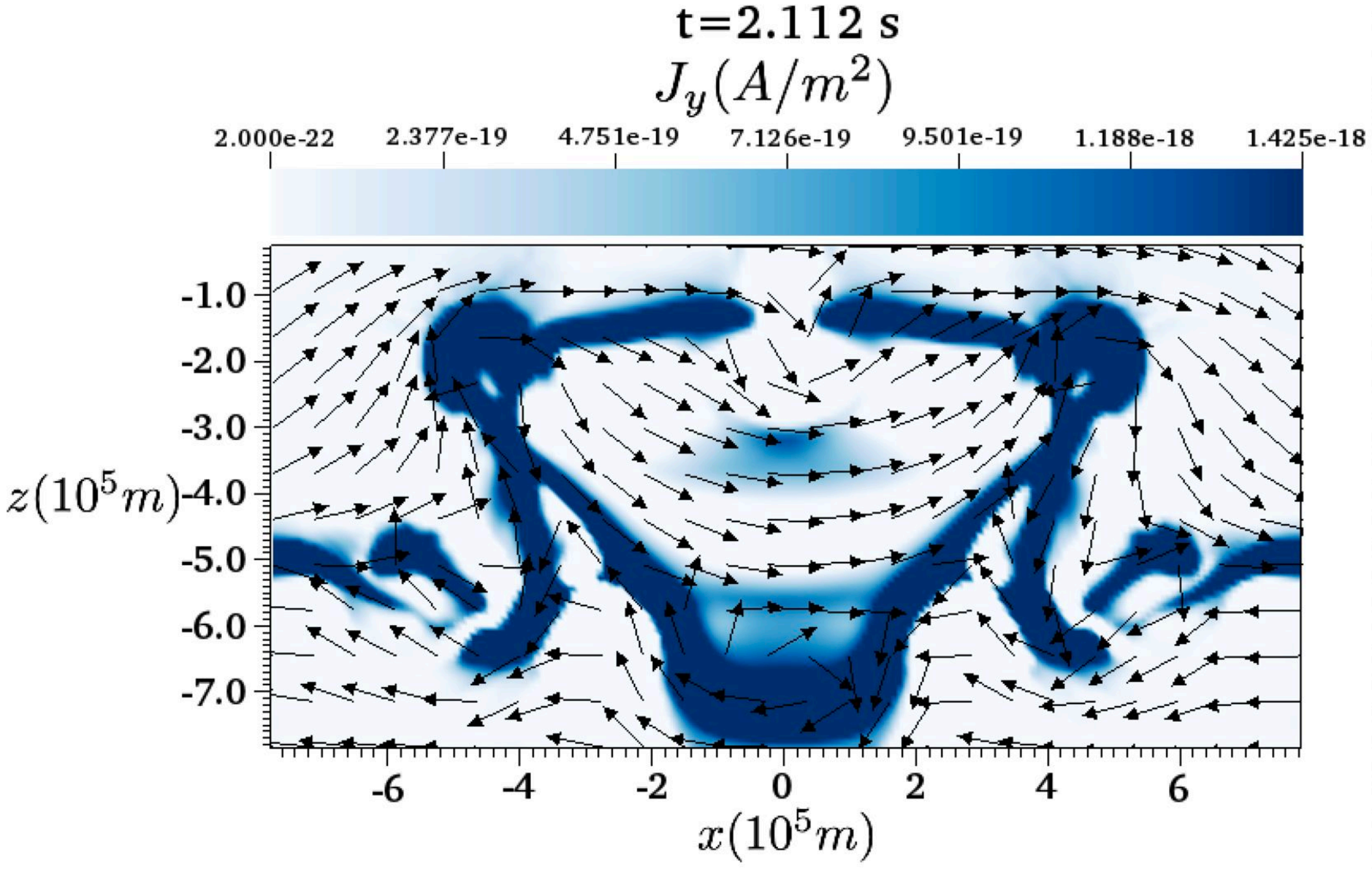

t=2.112 s
$J_y(A/m^2)$
2.000e-22
2.377e-19
4.751e-19
7.126e-19
9.501e-19
1.188e-18
1.425e-18
-1.0
-2.0
-3.0
$z(10^5m)$
-4.0
-5.0
-6.0
-7.0
-6
-4
-2
0
2
4
6
$x(10^5m)$

Fig3f.

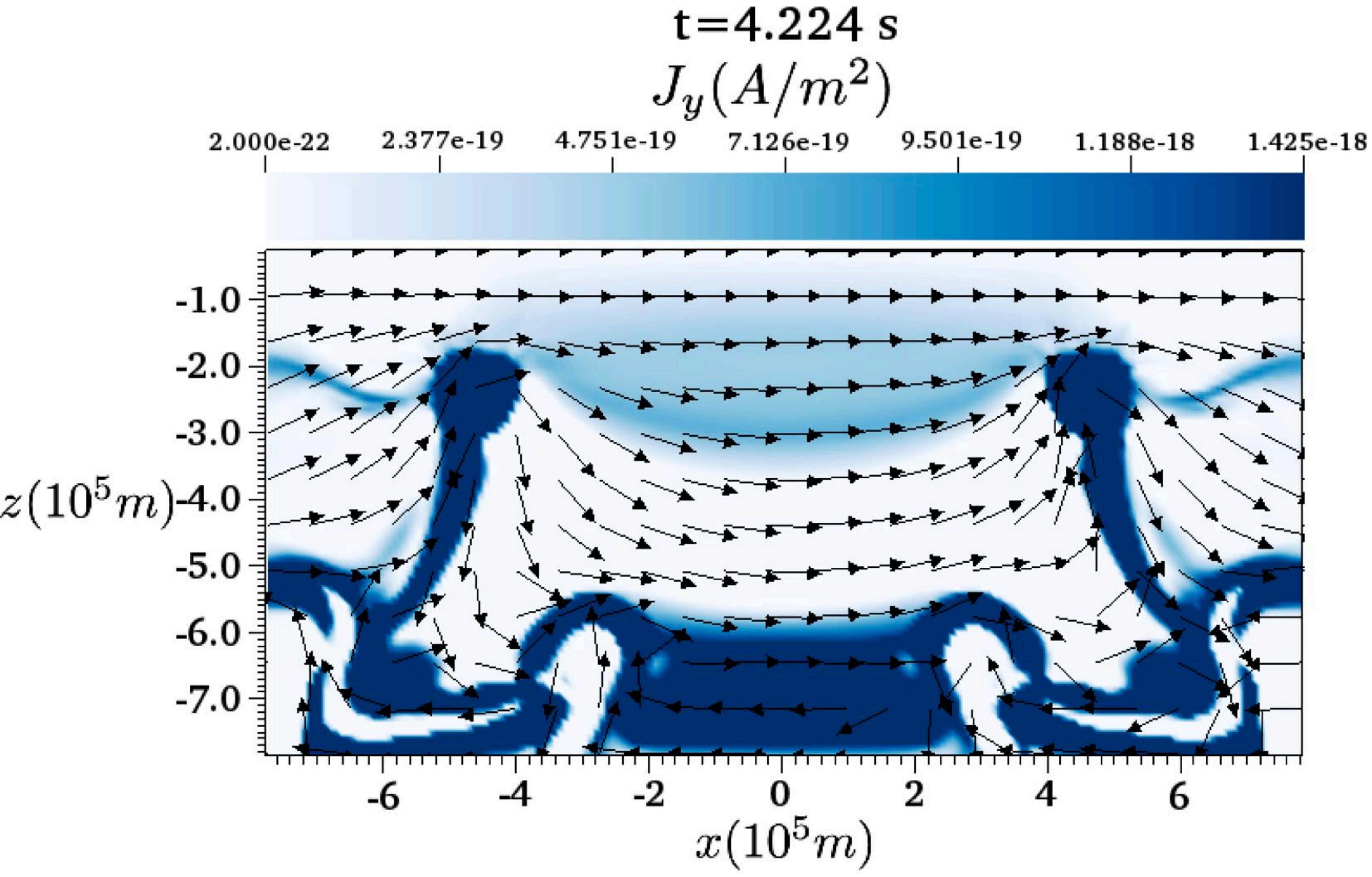
t=4.224 s
$J_y(A/m^2)$
2.000e-22
2.377e-19
4.751e-19
7.126e-19
9.501e-19
1.188e-18
1.425e-18
-1.0
-2.0
-3.0
-4.0
-5.0
-6.0
-7.0
$z(10^5m)$
-6
-4
-2
0
2
4
6
$x(10^5m)$

Fig3g.

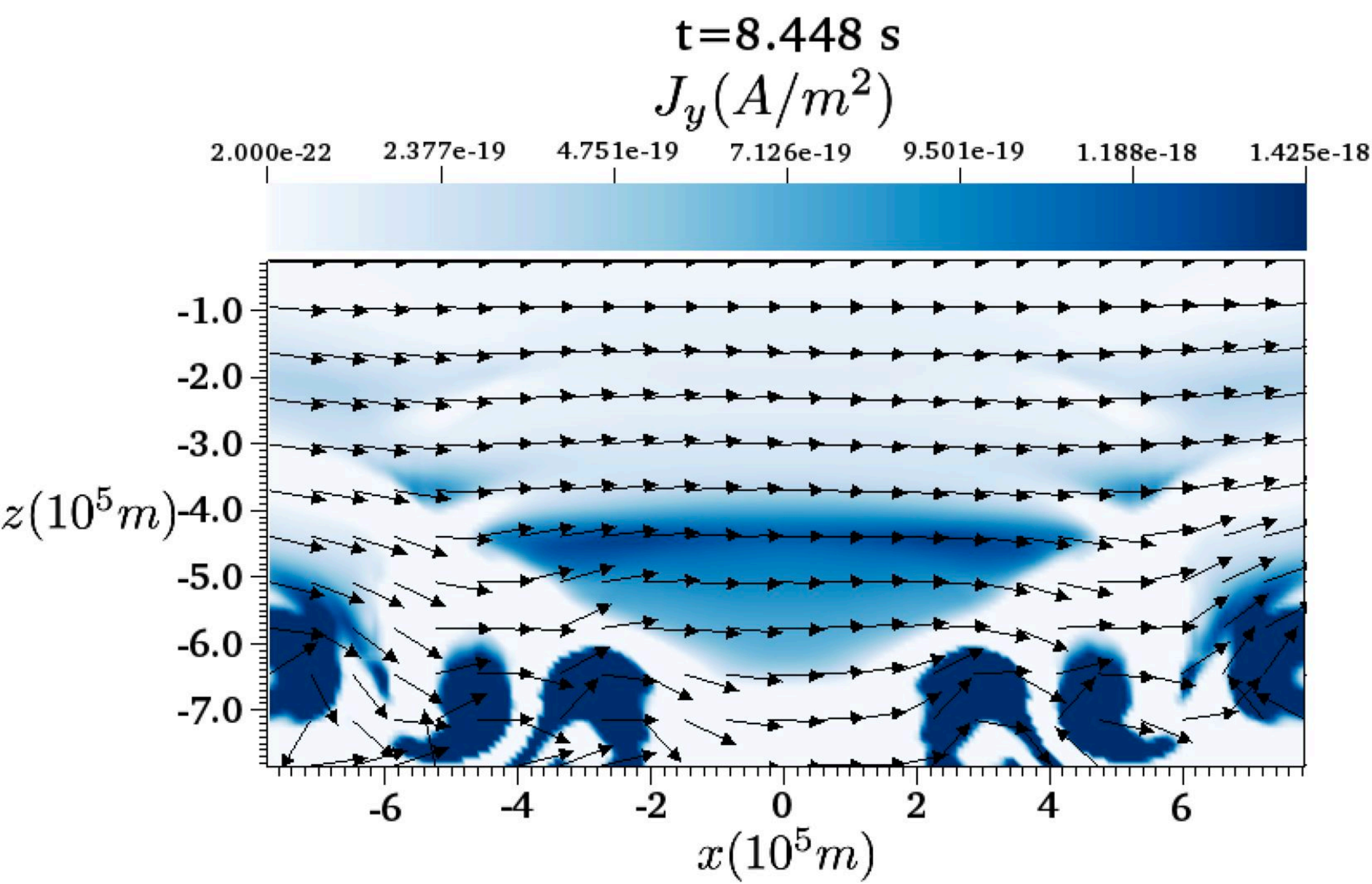

t=8.448 s
$J_y(A/m^2)$
2.000e-22
2.377e-19
4.751e-19
7.126e-19
9.501e-19
1.188e-18
1.425e-18
-1.0
-2.0
-3.0
$z(10^5m)$
-4.0
-5.0
-6.0
-7.0
-6
-4
-2
0
2
4
6
$x(10^5m)$

Fig3h.

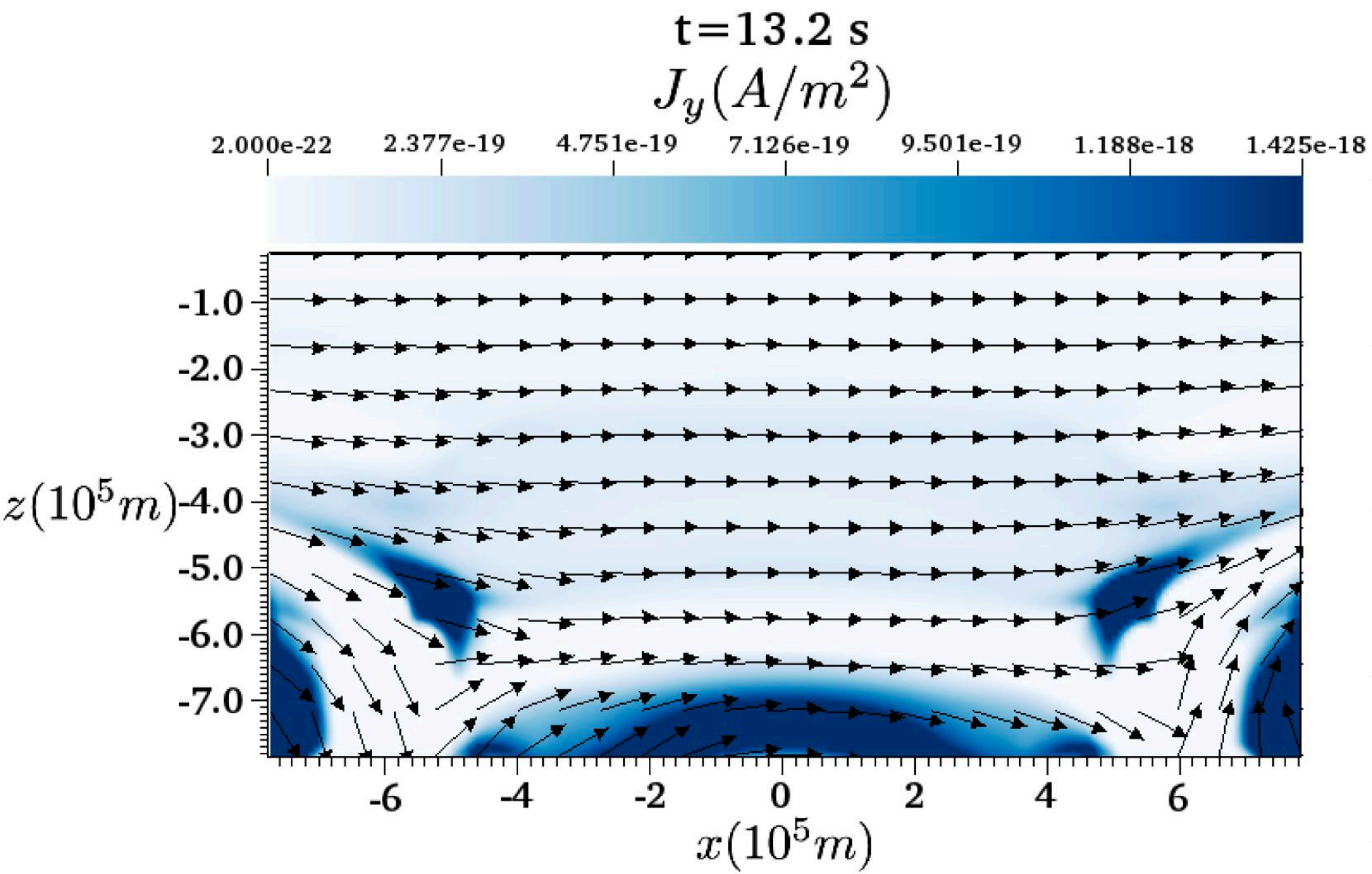

t=13.2 s
$J_y(A/m^2)$
2.000e-22
2.377e-19
4.751e-19
7.126e-19
9.501e-19
1.188e-18
1.425e-18
-1.0
-2.0
-3.0
-4.0
-5.0
-6.0
-7.0
$z(10^5m)$
-6
-4
-2
0
2
4
6
$x(10^5m)$

Fig4a.

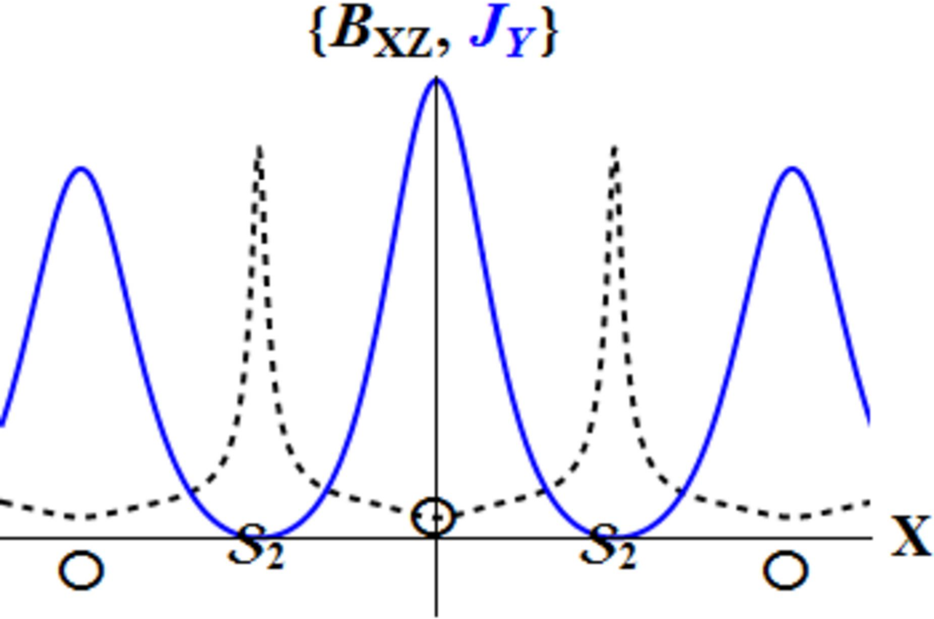

$\{B_{XZ}, J_Y\}$
X
O
S_2
S_2
O

Fig4b.

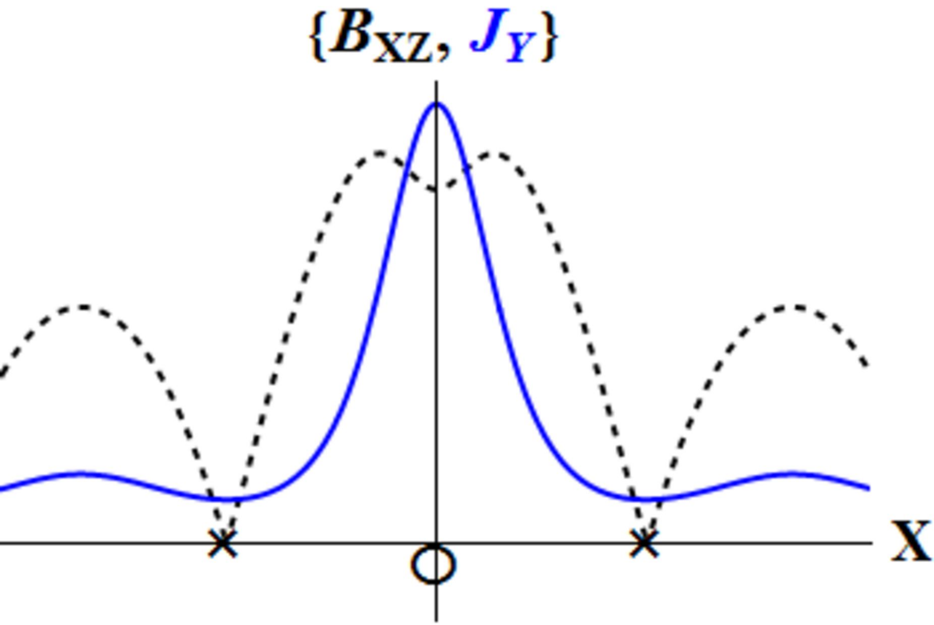
{B_{XZ}, J_Y}
X
O

Fig4c.

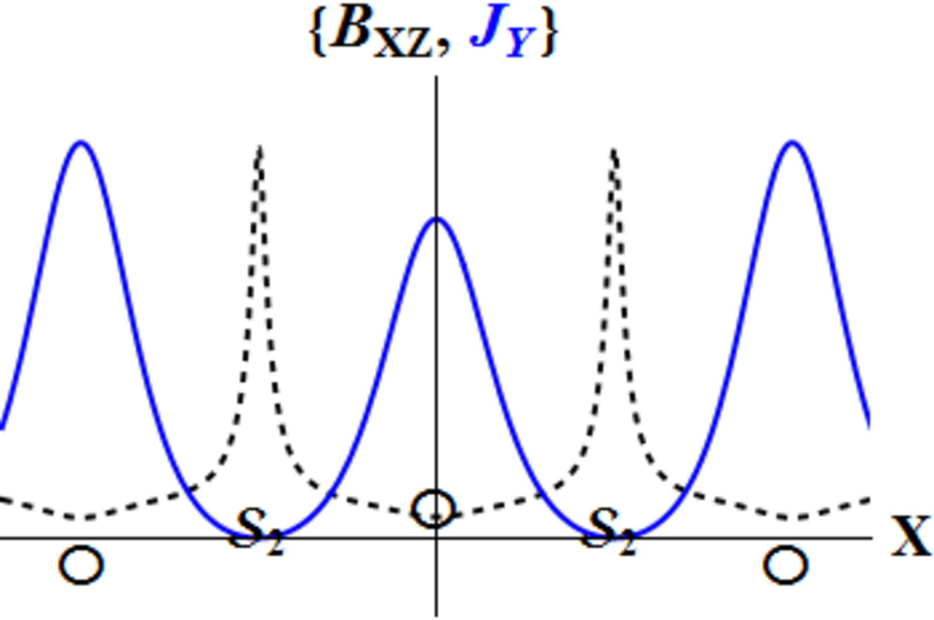
{B_{XZ}, J_Y}
X
O
S_2
O
S_2
O

Fig4d.

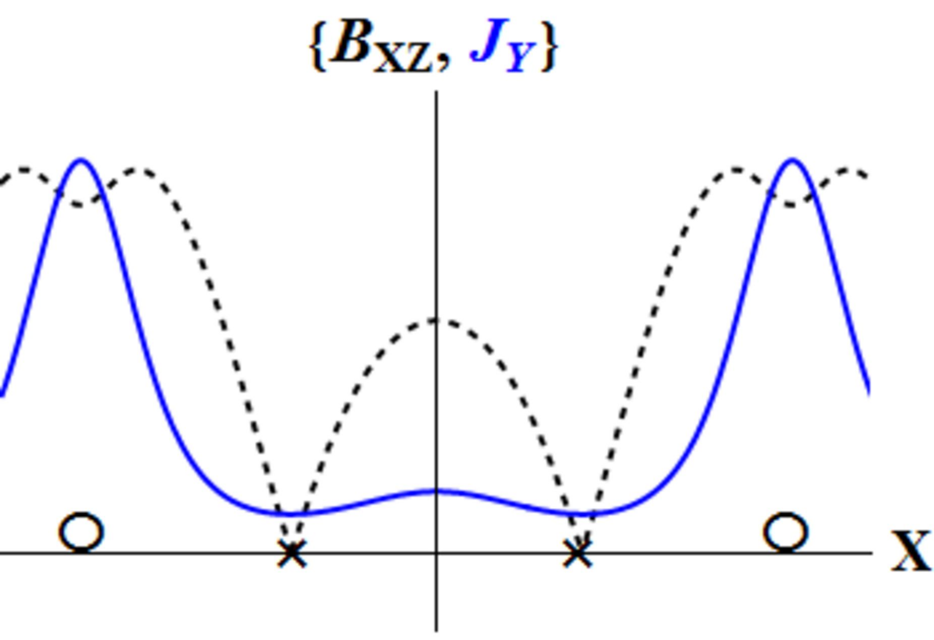

{B_{XZ}, J_Y}
X